THESIS FOR THE DEGREE OF LICENTIATE OF ENGINEERING

Advances in Absorption Processes for Nitrogen Oxides and Sulfur Oxides

Updated Mechanism for NO_2-Induced Sulfite Oxidation

ROSA CITRA APRILIA

Department of Environmental and Energy Sciences

CHALMERS UNIVERSITY OF TECHNOLOGY

Gothenburg, Sweden 2026

Advances in Absorption Processes for Nitrogen Oxides and Sulfur Oxides

Updated Mechanism for NO_2-Induced Sulfite Oxidation

ROSA CITRA APRILIA

Department of Environmental and Energy Sciences
Chalmers University of Technology
SE-412 96 Gothenburg
Sweden
Telephone +46(0)31-772 1000

Cover artwork by Azizah Inas Yandita. A monochromatic illustration depicting industrial flue gas plumes blending into the atmosphere, symbolizing the connection between anthropogenic emissions and the environment.

Printed by Chalmers Reproservice
Gothenburg, Sweden 2026

Advances in Absorption Processes for Nitrogen Oxides and Sulfur Oxides
Updated Mechanism for NO_2-Induced Sulfite Oxidation

ROSA CITRA APRILIA
Division of Energy Technology
Department of Environmental and Energy Sciences
Chalmers University of Technology

Abstract

Nitrogen oxides (NO_x) and sulfur oxides (SO_x) are hazardous air pollutants that are released primarily from combustion processes associated with power generation, industrial activities, and transportation. The best available technique (BAT) for handling these emissions from power generation and industrial processes involves two separate steps, applying selective catalytic reduction (SCR) for NO_x and limestone-based scrubbing for SO_x removal. While effective, this approach entails high investment and operational costs and constrains process flexibility due to the narrow temperature window of the catalyst. Absorption-based co-removal technologies are a promising alternative to remove both pollutants simultaneously under ambient conditions. However, a key challenge limiting commercial viability is the high consumption of sodium sulfite (Na_2SO_3), which is required to maintain satisfactory NO_2 absorption. The mechanism underlying the rapid depletion of sulfite in the presence of NO_2 and O_2 remains poorly characterized, with oxidation rates that vary significantly across studies and substantially exceed the reported kinetics.

This thesis addresses the knowledge gap related to the aqueous-phase chemistry governing the simultaneous absorption of NO_x and SO_x through kinetic and process modeling. In **Paper I**, five reaction sets are proposed to describe the rapid sulfite oxidation and the radical scavenging effect of thiosulfate observed in laboratory-scale experiments. The proposed mechanism shows good agreement with measurement data in terms of the liquid and gas-phase concentrations. In **Paper II**, the proposed mechanism is integrated into a process simulation, to evaluate process behavior under industrially relevant conditions. A sensitivity analysis identifies the inlet concentrations of NO_2 and sulfite as the key parameters governing process performance, with moderate impacts from mass transfer parameters. The findings contribute a new mechanistic understanding of sulfite oxidation kinetics and provide a basis for improved process design and control in absorption-based co-removal systems.

Keywords: Emissions control, absorption, nitrogen oxides, sulfur oxides, sulfite oxidation, thiosulfate, radical chain reaction, process modeling

List of publications

The thesis is based on the following appended papers, which are referred to in the text by their Roman numerals:

I. Aprilia, R.C.; Johansson, J.; Normann, F., Modeling Sulfite Oxidation Reactions in Co-Absorption of Nitrogen Oxides and Sulfur Oxides. Industrial & Engineering Chemistry Research, 2025. 64(51): p. 24516-24527.

II. Aprilia, R.C.; Johansson, J.; Normann, F., The Role of NO_2-Induced Sulfite Oxidation in Process Modeling of Nitrogen Oxides and Sulfur Oxides Absorption. Submitted for publication.

Author contributions

Rosa Citra Aprilia is the principal author of **Papers I** and **II**, responsible for the modeling, method development, result analysis, and writing of the papers. Dr. Jakob Johansson contributed to data curation, method development, and modeling support, as well as review and discussion of all papers. Prof. Fredrik Normann contributed to method development, modeling supervision, review and discussion of all papers.

Declaration of generative AI use

During the preparation of this work, the author used ChatGPT and Claude to refine the language, enhance clarity and readability, as well as perform initial screening of literature. It did not generate original scientific ideas, data, or conclusions. The author manually verified all literature, reviewed and edited the output as needed and took full responsibility for the content of the thesis.

Acknowledgments

The past 3 years have been an immensely rewarding period of academic growth which, to my surprise, has been an equally profound personal journey. It has been a privilege to pursue my studies in a nurturing and supportive environment, and I owe this experience to the many individuals who have shaped this journey.

First and foremost, I would like to express my gratitude to my supervisor, Fredrik Normann. Thank you for the fun ideas and enthusiasm you brought to discussions and meetings. Your guidance shaped not only this thesis but also the student writing it. My appreciation also goes to my co-supervisor, Jakob Johansson, your expertise has been foundational to this work. Thank you for sharing your knowledge, for the many hours you spent answering my questions and for providing an experimental perspective as a reality check.

I am also grateful to my colleagues in the Division of Energy Technology, for being a constant source of inspiration. To Anna and Katarina, for all the support you give relentlessly. To my colleagues in the High Temperature Process Group and Industrial Process Systems Group, for the feedback and discussions that have significantly improved the outcome of my work. I would also like to give a special shoutout to Farah, for being the kind friend that you are, and for offering a helping hand in my early days in the division.

My gratitude goes to "my village", who make it possible to juggle everything: My friends in and around Sweden, who make living on the other side of the world feel like a home away from home. My parents, for their endless support and prayers. My sisters, who have always been my 911, and who never fail to celebrate any of my achievements, no matter how modest they are.

To Lailana and Altan, I will never quite understand how such small humans can hold so much love (and energy!). Your daily supply of handcrafted gifts is the highlight of my days. You heal me and inspire me every day, and I will treasure the gifts for as long as they keep coming. To my better half, Alam, your kindness and patience have carried me through this PhD journey. Thank you for being my home through every season of life.

Finally, to everyone I met along the way, whose kindness and warmth made this journey brighter, please know that you made all the difference, and for that I am deeply grateful.

Rosa Citra Aprilia
Göteborg, Sweden
June 2026

Table of Contents

1. Introduction

Nitrogen oxides (NO_x) and sulfur oxides (SO_x) are hazardous air pollutants that are mainly released from anthropogenic sources. The presence of these acidic gases in the atmosphere has been linked to various health problems, with carcinogenic effects and pulmonary diseases as primary areas of concern[1]. The atmospheric reactions of NO_x have attracted attention, as it contributes to the formation of smog, which is a risk factor for respiratory infection that has increased since the COVID-19 pandemic[2, 3]. In addition, both oxide species are primary precursors for acid rain, which has been reported to cause deleterious effects on ecosystems, such as soil and freshwater acidification[4].

Globally, NO_x emission levels increased by a factor of six between 1970 and 2011, mostly from the power generation, industrial, and international shipping sectors[5]. This increase is mainly attributed to the rising emission levels across Asia and Africa, linked to economic growth and infrastructure development[6]. In Year 2011, NO_x emissions reached a turning point as China enforced more-stringent emissions control policies for coal power plants and industrial coal usage[3]. Meanwhile, in the US and Europe, NO_x emission levels had been declining since the 1990s, as a result of decreased coal consumption and the implementation of pollution control measures[7, 8]. Switching to low-sulfur fuels has proven to be effective at reducing SO_x emissions, as shown by the fuel shifts that occurred in the US and Europe in the 1990s, which contributed to a sustained global decline in emissions[5].

Today, a broader shift is ongoing as the global energy mix is transitioning towards sustainable energy sources in the pursuit of net-zero emissions. Although phasing out fossil fuel exerts a considerable impact on SO_x emissions, the usage of sustainable energy carriers, such as biomass[9] and hydrogen[10], may also contribute to NO_x formation. This suggests that transitioning away from fossil fuels will not in itself resolve the challenge of air pollution, as NO_x formation remains an intrinsic risk in high-temperature processes, regardless of fuel origin[10, 11]. Therefore, as the share of alternative fuels is projected to grow[12, 13], the need for a reliable technology to mitigate the associated emissions becomes increasingly crucial.

The best available technique (BATs) to reduce NO_x and SO_x emissions from power generation and industrial processes involves two separate steps, where selective catalytic reduction (SCR) and desulfurization with lime or sodium bicarbonate are applied to remove NO_x and SO_x, respectively[14, 15]. Despite SCR's high removal efficiency of 70%–95%, its performance is constrained by the catalyst's narrow and high temperature window (300°–

400°C) and the risk of ammonia slip[16]. High investment and maintenance costs have also been associated with the process, as the catalyst needs to be replaced periodically[17].

There is good potential for absorption-based co-removal technologies for NO_x and SO_x, as they offer levels of NO_2 absorption that are comparable to those of SCR, while removing both pollutants in a single step[18]. They also have the advantage of operating under ambient conditions with flexible flue gas loads[19]. The challenge associated with the removal of NO_x through absorption is the low solubility of NO, its primary constituent, which is mitigated by applying an oxidizing step to obtain the more-soluble NO_2[20]. This process also generates a nitrogen- and sulfur-rich effluent, which raises environmental issues when discharged without prior treatment[21, 22]. A key challenge addressed in this thesis is the high level of consumption of sodium sulfite (Na_2SO_3), which is required to ensure a satisfactory level of NO_2 removal[23]. The dynamics linked to the depletion of S(IV) ions (SO_3^{2-} and HSO_3^-) and NO_2 absorption has been poorly characterized, yielding different apparent rates between studies[24-26], and is significantly faster than the reported kinetics of S(IV) oxidation[27-29]. Radical scavengers, such as thiosulfate salts ($Na_2S_2O_3$), have been shown to minimize chemical consumption and show promising improvements in process efficiencies[24, 30], although the specific radical scavenging mechanism remains to be established[30].

Resolving the issue of high chemical throughput is the key to advancing the process to commercial viability. Therefore, it is essential to address the knowledge gap in the underlying chemistry, as this would provide a better understanding of how species interact within the system and influence process performance. A detailed insight into the reaction mechanism would also facilitate reliable process design and control, which are important aspects in the scaling up of the process.

1.1 Aims and scope

This thesis aims to characterize the aqueous-phase chemistry governing the simultaneous absorption of NO_x and SO_x. The focus is on the oxidation of S(IV) in the presence of gaseous NO_2 and O_2 and the radical scavenging mechanism of thiosulfate ($S_2O_3^{2-}$). New reaction sets and their kinetic expressions are formulated by combining available empirical data and modeling results, aimed at addressing the rapid depletion of S(IV). The obtained mechanism is then applied to evaluate process behaviors under different operating conditions.

The work is structured around the following topics:

1. S(IV) consumption rates across commercial and experimental setups.
2. Identification of the radical scavenging mechanism of thiosulfate.

3. Evaluation of process performance to establish the key process parameters.

The work centers on the absorption process following separate oxidation of NO, in which NO_2 is considered to be the sole product and SO_2 is assumed to be the sole component of SO_x. The process operates at ambient pressure and under alkaline conditions.

1.2 Thesis outline

The thesis consists of an introductory essay that contextualizes the work within the current state of the art. The thesis is based on the two appended papers, which can be briefly summarized as follows:

Paper I presents the result of a kinetic modeling work, whereby five reaction sets are proposed to describe the rapid S(IV) oxidation and thiosulfate scavenging mechanism in a laboratory-scale experiment.

Paper II applies the proposed mechanism in a process modeling simulation, to evaluate the process behavior and identify the key operating parameters.

2 Background

2.1 Air pollution

Air pollution refers to the presence of harmful substances in the atmosphere at concentrations that are sufficient to damage human health, ecosystems or the climate system. It is now firmly established as the single largest environmental health risk worldwide[31]. The World Health Organization estimates that the combined effects of ambient (outdoor) and household air pollution caused 6.7 million premature deaths in 2019, predominantly from cardiovascular disease, stroke, chronic obstructive pulmonary disease (COPD), lung cancer, and acute respiratory infections[31]. A growing body of evidence links air pollution to additional outcomes, including low birth weight, diabetes, cognitive impairment, and mental health problems[32]. Furthermore, these impacts are not evenly distributed, as they fall disproportionately on the most-vulnerable groups, such as children, for whom exposure can cause lasting developmental harm, as well as people with pre-existing conditions, older persons, and those in poorer socio-economic circumstances[33].

The primary pollutants with the strongest linkages to public health concerns are particulate matter (PM), carbon monoxide (CO), ozone (O_3), nitrogen dioxide (NO_2), and sulfur dioxide (SO_2)[34]. Several of these damaging species are not emitted directly, but are formed in the atmosphere and referred to as *secondary pollutants*. Reactions between primary pollutants such as NO_2, SO_2, and solar radiation produce secondary pollutants, including ground-level O_3, which is formed when NO_2 reacts with volatile organic compounds (VOCs) under sunlight, and fine sulfate and nitrate aerosols ($PM_{2.5}$), which are formed when SO_2 and NO_2 react with ammonia and water vapor[35, 36]. Fine PM is a particularly important source of risk, as these small particles penetrate deep into the lungs, enter the bloodstream, and reach organs, causing systemic damage to tissues and cells[37].

The harm extends beyond human health, as both NO_x and SO_x drive acid deposition, acidifying soils and freshwater bodies, and contributing to eutrophication through reactive nitrogen deposition[38, 39]. The significant contributions from NO_x and SO_x define the focus of the present study, as their mitigation would reduce the subsequent formation of secondary $PM_{2.5}$ and O_3. These oxides are the principal species targeted by international and regional emissions-reduction frameworks, including the Convention on Long-Range Transboundary Air Pollution and its Gothenburg Protocol.

2.2 NO_x and SO_x emissions sources

Global levels of NO_x and SO_x emissions have risen steadily with economic growth. Heavy industry, coal-fired electricity generation, and rapidly expanding automobile fleets drove emissions rates upwards throughout the 1950s and 1960s[40]. The sources of NO_x and SO_x emissions today are distributed across several major sectors (Figure 1), with significant regional variation depending on the state of economic development and environmental regulation.

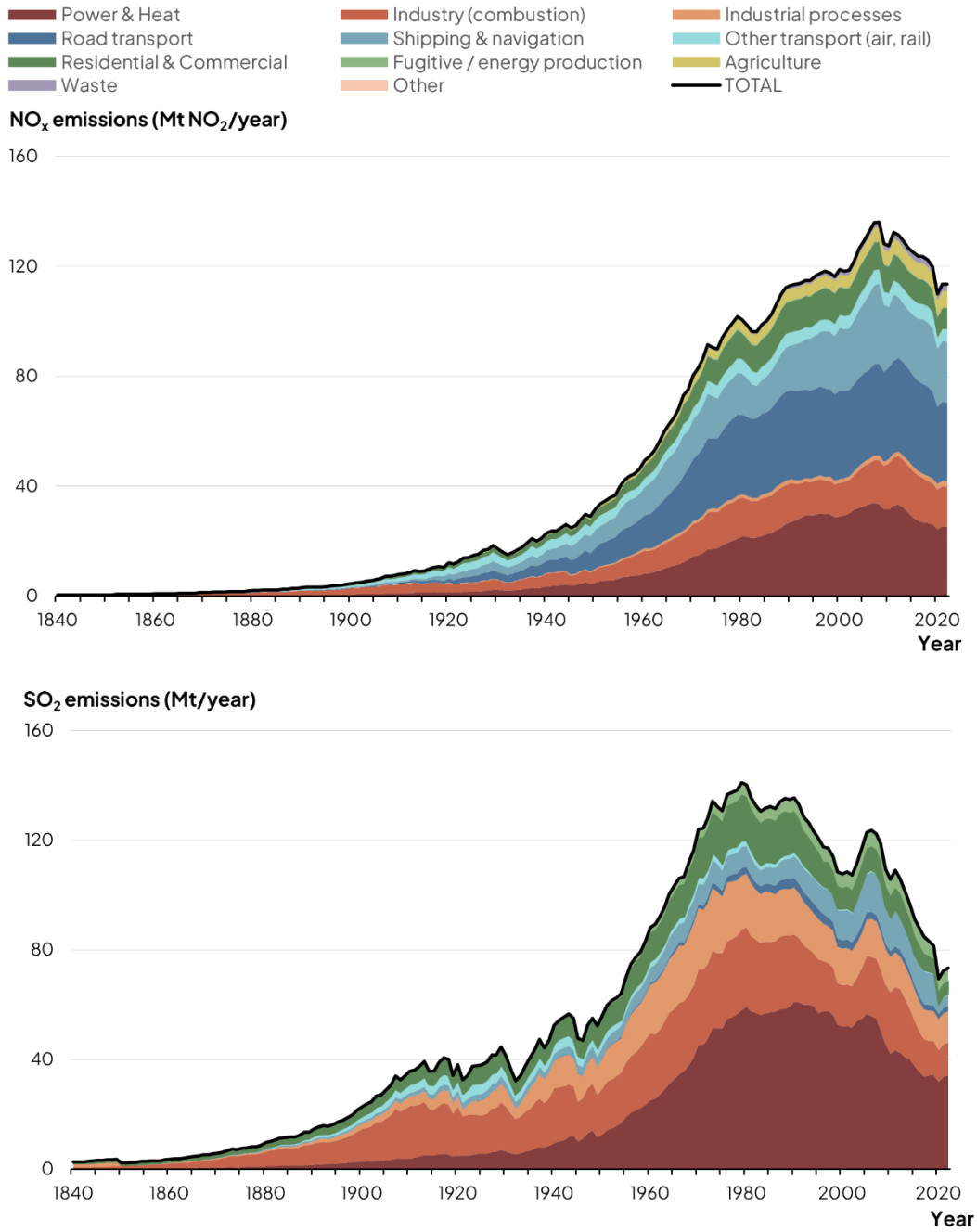

Figure 1 *Global anthropogenic emissions of NO_x (top panel) and SO_2 (bottom panel) by sector. 'Shipping and navigation' refers to international shipping and domestic navigation. Full descriptions of the sectors are available in the Community Emissions Data System, 2024 version[40].*

Electricity generation remains the single largest source of SO_x globally and is a major source of NO_x. The continued construction of new coal capacity in South and Southeast Asia to meet rapidly growing electricity demand means that the power sector will remain a dominant source of these emissions for decades to come.

Road transport is currently the main source of NO_x emissions in most countries, and is a significant contributor globally. Internal combustion engines, diesel engines in particular, work at high temperatures which generate substantial levels of thermal NO_x. In the US, road vehicles accounted for nearly one-quarter of NO_x emissions in Year 2023[41]. The past two decades have seen major regulatory efforts to reduce vehicle NO_x emissions through progressively stringent emissions standards (Euro standards in the EU; Tier standards in the US; China's national standards). Electrification of road transport is structurally the most significant near-term measure in NO_x emissions reduction. In Year 2025, one in four new cars sold globally was electric[42], and electric vehicle penetration is accelerating in Europe, China, and the US, while heavy-duty trucks remain a more-intractable challenge. Road transport has become a negligible source of SO_x following the widespread adoption of ultra-low-sulfur diesel and petrol (≤15 mg/kg sulfur) in most major markets[43-45].

International maritime shipping is a substantial source of both NO_x and SO_x. The global shipping fleet burns primarily heavy fuel oil (HFO), which was historically unregulated and could contain up to 4.5% sulfur by mass, which is roughly 4,500-times the current sulfur limit for road diesel[46]. Given the sector's fuel consumption of approximately 250–300 million tons per year, maritime shipping is a substantial source of both pollutants, accounting in Year 2012 for roughly 17% of global anthropogenic NO_x and 11% of global SO_x emissions[40].

Figure 2 shows the progression of the marine-fuel sulfur limit under the International Maritime Organization (IMO) MARPOL Annex VI[47]. A landmark regulatory change came into effect on January 1, 2020, when the IMO reduced the global cap on sulfur in marine fuel from 3.5% to 0.5% by mass. The new rule led to a rapid decline in shipping-related SO_2 emissions. However, compliance relies on either switching to low-sulfur fuel oil (LSFO) or the installation of exhaust gas cleaning systems (scrubbers) on ships that are burning HFO, which has been criticized as simply transferring the pollution from the exhaust gas to the ocean, as open-loop scrubber effluents are discharged into the ocean[21, 22].

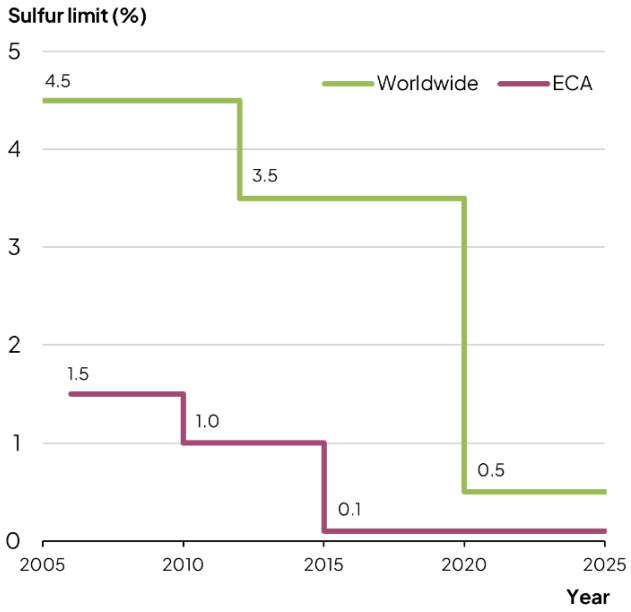

Figure 2 *Marine-fuel sulfur limit progression applied worldwide and in the Emission Control Areas (ECAs)*

The levels of NO_x emissions are regulated through the IMO's Tier system[47]. Tier II (from Year 2011 onwards) applies globally, while the more-stringent Tier III standard, which requires an 80% reduction in NO_x relative to Tier I, applies only to vessels constructed from Year 2016 onwards operating in the designated Emission Control Areas (ECAs)[47]. Despite the increasingly stringent regulations, real-world measurements of ship NO_x emissions have revealed concerning gaps: measurements performed on 545 ships in Danish waters showed no statistically significant difference in NO_x emission rates between unregulated Tier 0 engines and the supposedly more-stringent Tier II engines, indicating a substantial gap between regulation and practice[48]. Shipping traffic is projected to grow with global trade, which means that in the absence of further regulatory action, shipping will account for an increasingly prominent share of global NO_x as other sectors decline.

Heavy industry remains a persistent source of both NO_x and SO_x emissions, especially in industrializing economies. Key sectors include iron and steel, cement, refineries and chemical plants, pulp and paper mills, and glass manufacturing. The two pollutants originate from fundamentally different sources, and this distinction dictates the abatement challenge. NO_x is predominantly formed through the dominant thermal route described by the extended Zeldovich mechanism[10]. This mechanism proceeds through the dissociation and recombination of atmospheric N_2 and O_2, which accelerates exponentially with temperature[10], with secondary contributions from fuel-bound nitrogen and prompt NO_x[49]. As high temperatures are required for processes such as clinkering, glass melting, and metal reheating, NO_x reduction approaches are heavily process-dependent. Meanwhile, SO_2 is essentially a feedstock-derived pollutant,

arising from the sulfur already bound within the fuel or the raw materials, such as in the roasting of sulfide ores and the sulfur content of cement raw meal[50, 51]. As the sulfur mass balance is conserved throughout the process, the SO_2 output is approximately proportional to the sulfur input and cannot be suppressed by adjusting the combustion conditions alone.

Regulatory controls for SO_x and NO_x from industrial sources vary widely across the globe. The European Union regulates large combustion and industrial installations through the Industrial Emissions Directive (IED), under which permitted limits are tied to the performance levels associated with best available techniques (BAT) rather than to fixed statutory values[1]. The US instead couples technology-based New Source Performance Standards[52] under the Clean Air Act with a market-based allowance-trading scheme for SO_2[53], while China enforces "ultra-low emission" concentration ceilings, which are currently among the most-stringent worldwide[54, 55]. Elsewhere, the regulations are considerably more permissive, with several administrations setting limits that are an order of magnitude higher or that, for particular sectors, impose no ceiling at all.

Looking forward, the landscape of NO_x and SO_x sources will be shaped by the energy transition, industrial growth, and the deployment of pollution control technologies. Natural gas, which acts as a bridge fuel during the energy transition, produces a negligible level of SO_2 but a substantial amount of NO_x[56]. Hydrogen combustion, which is often promoted as a clean alternative, presents a significant NO_x risk due to its high-temperature conditions, which increase thermal NO_x formation[57]. In the international shipping sector, the IMO's 2023 revised greenhouse gas strategy, which targets net-zero shipping emissions around Year 2050[55], will require a shift to alternative fuels (methanol, ammonia, hydrogen, LNG) that will also reshape the NO_x and SO_x profiles of the sector, as none of the available alternatives is entirely without NO_x concerns.

2.3 Best available techniques for NO_x and SO_x removal

Mitigation measures for NO_x and SO_x emissions across industrial sectors involve BATs, which establish proven and economically viable abatement methods to meet the emissions limits set out in regulations such as the EU Industrial Emissions Directive. Although the processes involved differ substantially between sectors, the control strategy is consistent and follows a three-step approach:

1. Preventive measures, primarily involving the selection of fuels and raw materials with low nitrogen and sulfur contents;
2. Primary measures that suppress pollutant formation during combustion; and

3. Secondary measures that remove the pollutant from the flue gas after it has formed.

Secondary measures generally achieve the highest removal efficiencies, although they are capital-intensive and entail a significant environmental trade-off.

The control of NO_x is shaped by the mechanisms of its formation. The majority of industrial NO_x emissions originate either from thermally induced oxidation of atmospheric nitrogen or from oxidation of nitrogen bound within fuels. Thus, primary measures are designed to lower the peak flame temperature and to stage the introduction of air or fuel, such that no combustion zone is simultaneously hot and oxygen-rich. Techniques such as low-NO_x burners, air and fuel staging, and flue gas recirculation are widely applied across the power, cement, glass, and refining sectors[14, 51]. Meanwhile, oxy-fuel combustion, which removes atmospheric nitrogen from the combustion environment, has found particular application in glass manufacturing[58]. The effectiveness of these measures is limited by a trade-off between NO_x suppression and the completeness of combustion, as the same conditions that inhibit NO_x formation tend to increase emissions of carbon monoxide and unburnt carbon. Consequently, primary measures can lower NO_x only to a certain level before the combustion efficiency is compromised, which necessitates the use of secondary techniques when stricter limits apply. The principal primary measures, together with their fields of application and characteristic limitations, are summarized in Table 1.

Table 1 *Primary (combustion-stage) measures for NO_x control.*

Technique	Mechanism	Principal fields of application	Limitation(s)
Low-NO_x burners	Internal staging of air and fuel lowers peak flame temperatures, and establishes fuel-rich zones	Power, cement, glass, refining, lime kilns	Modest reduction in isolation; increases levels of CO and unburnt carbon
Air staging	Combustion in furnace/boiler divided by a primary and secondary addition of air	Power, cement, recovery boilers	Risk of incomplete combustion; constrained by furnace geometry
Fuel staging / reburning	Downstream secondary fuel injection creates a reduction zone that may convert formed NO_x to N_2	Power, cement (mid-kiln firing)	Requires a suitable secondary fuel and residence time
Flue gas recirculation	Recirculated gas dilutes oxygen and lowers flame temperatures	Power (gas), glass	Effective mainly for gaseous fuels; affects flame stability
Combustion optimization	Computerized control of the air-to-fuel ratio to maintain near the optimum	All sectors	Limited reduction when used alone; foundational rather than sufficient
Oxy-fuel combustion	Combustion in near-pure oxygen removes atmospheric nitrogen, suppressing thermal NO_x	Glass	Requires high oxygen supply; energy cost; major furnace redesign

Among the secondary techniques for NO_x control, SCR achieves the highest performance, reducing NO_x emissions by 70%–95% through the reaction of injected ammonia or urea over a catalyst at temperatures in the range of 300°–400°C. It is the most widely deployed end-of-pipe NO_x control measure worldwide, with more than 1,400 power plants reported to employ it as of Year 2014, distributed mainly across North America, Asia, and Europe[14]. Its configuration is dictated by the composition of the flue gas, as power plants have the catalyst typically installed upstream of the dust removal and desulfurization step, where the gas temperature is naturally suitable such that reheating can be avoided. Meanwhile, in dustier or more-corrosive streams, such as those encountered during iron and steel production, the catalyst is placed downstream of dedusting and desulfurization in order to protect it, at the expense of reheating the gas back to its operating temperature. The principal limitations of SCR are economic and operational. The catalyst has a finite lifetime, typically 3–7 years in coal-fired units or longer in oil and gas-fired units, after which it must be regenerated or discarded. It is also susceptible to deactivation by fly ash and catalyst poisons, poses a risk of ammonia slip, and oxidizes a small fraction of SO_2 to SO_3, which promotes corrosion and fouling in downstream equipment.

Table 2 *Comparison of selective catalytic reduction (SCR) and selective non-catalytic reduction (SNCR) processes.*

Characteristic	SCR	SNCR
NO_x reduction	70%–95%	30%–60%
Operating temperature	300°–400°C	850°–1,000°C (ammonia); 800°–1,100°C (urea)
Catalyst	Required; lifetimes of 3–7 years (coal) to 8–12 years (oil and gas)	None
Ammonia slip	Lower; the catalyst completes the reaction	Higher; the reagent must be supplied in excess
Space and retrofit	Substantial; reactor and possible gas reheating	Compact and readily installed
Dominant cost	Catalyst procurement and management	Reagent consumption
Principal cross-media penalty	Oxidation of SO_2 to SO_3, spent catalyst as waste	Ammonia slip; possible N_2O formation
Application	Large or new plants subject to strict limits	Cement kilns; mid-sized units; low-cost retrofit

Selective non-catalytic reduction (SNCR) offers a simpler and less-costly alternative, achieving NO_x reductions of 30%–60% by injecting ammonia or urea directly into the furnace in the absence of a catalyst. The reaction proceeds only within a narrow temperature range (approximately 850°–1,000°C for ammonia and 800°–1,100°C for urea), above which the reagent is itself oxidized to produce additional NO_x, and below which conversion is incomplete and the reagent escapes unreacted. The technique is particularly well-suited to cement kilns, as the kiln gas naturally operates within the required temperature range, and to mid-sized boilers for which the strict limits that justify SCR do not apply. To achieve higher levels of NO_x reduction, an additional catalyst layer is installed downstream of an SNCR stage, to complete the reduction process and to limit the ammonia slip, thereby capturing part of the performance of SCR at a reduced cost[14]. The characteristics of the two secondary techniques are compared in Table 2.

In contrast to NO_x, SO_x levels cannot be suppressed by modifying the combustion conditions, as the sulfur present in the fuel or raw material is conserved and must, therefore, either be excluded at the input or captured from the flue gas. Beyond the preventive selection of low-sulfur inputs, control relies on the activities of scrubbing technologies. Dry sorbent injection, in which lime or limestone is introduced into the furnace or duct, represents the simplest and least-efficient option, followed by semi-dry systems such as spray dry absorbers and circulating

fluidized bed scrubbers[59]. Wet flue gas desulfurization (WFGD), in which a limestone slurry absorbs SO_2 within a scrubber tower, constitutes the benchmark for large combustion plants, owing to its removal efficiency of 95% and the production of gypsum as a saleable byproduct. These advantages are, however, offset by a substantial capital cost, the generation of a wastewater stream that requires treatment, and a measurable reduction in the net energy efficiency of the plant. The SO_x control techniques, ordered by increasing capture efficiency and cost, are presented in Table 3.

Table 3 *Techniques for SO_x control, in order of increasing capture efficiency and cost.*

Technique	**Mechanism**	**Capture rate**	**Principal fields of application**	**Limitation(s)**
Fuel and raw-material sulfur control	Selection of low-sulfur coal, oil, coke, ore, or cement raw meal	-	All sectors	Availability and cost of low-sulfur inputs
Dry sorbent injection	Dry lime or limestone injected into the furnace or duct	Low to moderate	Power, cement, sinter	Poor sorbent utilization; mixed dry residue
Spray dry absorber	Lime slurry sprayed into the hot gas and dried to a powder	Moderate to high	Power, cement	Dry residue rather than saleable gypsum
Circulating fluidized bed scrubber	Recirculated sorbent for high utilization	High	Power	Solid-waste handling; space
WFGD	Limestone slurry used to absorb SO_2 in a scrubber tower	Very high (>95%)	Power (predominant), refining	High capital cost; wastewater; energy penalty
Alkaline / wet scrubbing	Caustic or lime scrubbing of acid gases	High	Sinter, pulp kilns and Total Reduced Sulfur (TRS) burners, glass	Effluent generation; reagent cost
Regenerative activated carbon	Adsorbs SO_2 (with NO_x and dust); regenerated to yield sulfuric acid or sulfur	High, multi-pollutant	Sinter plants, power (combined)	High cost; limited deployment

Among the emerging techniques covered in the BAT reference documents is the simultaneous removal of NO_x and SO_x within a single system, which resolves the SO_2 oxidation problem in an SCR unit following WFGD. The regenerative activated carbon process, in which SO_2 is adsorbed as sulfuric acid and NO_x is subsequently reduced catalytically, has been adopted as a BAT for sinter plants in the iron and steel sector, where the presence of multiple pollutants in the off-gas makes it an especially attractive option. However, the wider adoption of this technology has been constrained by cost, so it remains restricted to a low number of installations.

In the BAT framework, the determination of a suitable strategy is made for each installation rather than universally, as the optimal choice reflects a balance between the targeted level of reduction and the availability of resources at a specific site. Therefore, the present work aims to create the basis for further process evaluation of absorption-based simultaneous removal, which mitigates the problems associated with a sequential separation process.

2.4 Simultaneous removal of NO_x and SO_x

The major constraint of removing both pollutants is the large fraction of chemically inert NO, which accounts for 90%–95% of the NO_x. Therefore, the success of a co-removal process relies on the conversion of NO to a more-reactive species, such as NO_2, N_2O_5, HNO_2 or HNO_3. The following section explores four distinct process families that are currently being developed for the simultaneous removal of NO_x and SO_x. Table 4 maps out the relevant processes, as well as their active components, removal efficiencies, maturity levels, and the key challenges.

Table 4 *Process families for simultaneous NO_x and SO_x removal, grouped according to contacting regime (dry, semi-dry, wet), with active components, commercial name, typical NO_x and SO_2 removal levels, maturity, byproducts and main challenges.*

Process family	Active component	Commercial name	NO_x removal	SO_2 removal	Maturity	Byproduct	Main challenge	Ref.
Dry processes								
Adsorption–catalysis	Regenerable activated carbon or activated coke (char)	Bergbau-Forschung/Uhde/Mitsui-BF	60%–80%	95%–98%	Commercial	Recovered elemental sulfur or H_2SO_4	Carbon attrition and consumption; large adsorber volume; regeneration energy requirement	60
Combined catalytic oxidation–reduction	V_2O_5–WO_3/TiO_2 SCR catalyst; V_2O_5–$M_2S_2O_7$/SiO_2 DeSOx catalyst (M=K, Na, Cs)	SNOX; DESONOx	~94%	>95%	Commercial	Concentrated saleable H_2SO_4	High capital cost; catalyst cost and replacement	61,62
Catalytic baghouse (sorbent + SCR)	Hydrated lime or $NaHCO_3$ sorbent + SCR catalyst + NH_3	SOx–NOx–Rox Box (SNRB; Babcock & Wilcox)	80%–90%	70%–90%	Demonstration (5 MWe)	Dry $CaSO_4$/$CaSO_3$ (or Na_2SO_4); spent sorbent	High-temperature bag durability; inefficient sorbent utilization	63
Regenerable metal-oxide sorbent	CuO on Al_2O_3 (adsorbs SO_2; catalyzes NH_3-SCR) and SCR catalyst	Copper-oxide process	90%–95%	81%–96%	Demonstration	H_2SO_4 or sulfur upon regeneration	Sorbent regeneration/consumption; reductant consumption; high-temperature duty	64, 65
Supported alkali sorbent	Na_2CO_3 / $NaHCO_3$ on γ-alumina	NOXSO process	70%–90%	>90%	Pilot / demonstration	H_2SO_4 or sulfur	Sorbent regeneration and process complexity	66, 67
Electron-beam irradiation	High-energy electrons + NH_3 → $(NH_4)_2SO_4$ + NH_4NO_3	Electron-beam ammonia (EBA); EBARA / EBFGT	70%–95%	>90%	Demonstration to commercial	Ammonium sulfate / nitrate salts	High electricity demand; electron-gun reliability	68, 69
Non-thermal plasma	Plasma-generated radicals + NH_3	N/A	50%–80%	80%–98%	Laboratory / pilot	Ammonium sulfate / nitrate salts	High energy consumption; equipment reliability; limited scale-up	70, 71

Process family	Active component	Commercial name	NO_x removal	SO_2 removal	Maturity	Byproduct	Main challenge	Ref.
Semi-dry processes								
Spray-dryer absorption (+ oxidant for NO_x)	Atomized lime slurry $Ca(OH)_2$; oxidant for NO	N/A	60%–90%	67%–97%	Laboratory	Dry mixed Ca sulfite/sulfate/nitrate	Limited NO_x removal without added oxidant; solid-waste disposal	72, 73
Circulating dry scrubber (CDS)	Hydrated lime in a circulating fluidized bed; NO oxidant (Ferrate(VI), O_3)	N/A	67%	96%	Laboratory	Dry mixed Ca sulfite/sulfate/nitrate	Inefficient sorbent utilization; solid-waste disposal	74, 75
Wet processes								
Gas-phase ozone oxidation + wet scrubbing	Ozone for NO oxidation; limestone/lime or NaOH solution	LoTOx (Linde, formerly BOC)	up to 95%	up to 98%	Commercial	Nitric acid / nitrates + gypsum	Ozone generation energy and cost; ozone slip	76, 77
Oxidant-enhanced WFGD	$NaClO_2$ / NaClO / ClO_2 / H_2O_2 / $KMnO_4$ for NO oxidation; wet $CaCO_3$	N/A	34%–70%	~100%	Pilot- to full-scale trials	Mixed sulfate/nitrate; chloride-laden wastewater	Oxidant cost; chloride wastewater treatment	78, 79
Sulfite / alkali co-absorption	Gaseous oxidant for NO; Na_2SO_3 for S(IV) absorbent	N/A	70%–90%	>95%	Research / developing	Sulfate and nitrogen salts in effluent	High S(IV) consumption; nitrogen/sulfur effluent treatment	80
Ammonia scrubbing	Gaseous oxidant for NO; Aqueous NH_3 → $(NH_4)_2SO_4$ / NH_4NO_3	N/A	60%–90%	~99%	Laboratory	Ammonium sulfate / nitrate fertilizer	Ammonia slip and aerosol formation	81
Pressurized oxidative absorption	O_2 under pressure + water (lead-chamber chemistry)	Sour compression / CO_2CPU (Air Products)	70%–90%	90%–99%	Pilot (oxy-fuel CCS)	Mixed H_2SO_4 / HNO_3 acids	Requires high pressure; acid corrosion (316L); SO_2–NO_x interference	82, 83

Removal levels are typical reported ranges and depend strongly on configuration, reagent dose and operating conditions; the SNRB and pressurized-absorption figures are from the cited pilot studies, the LoTOx figure is from vendor data, and the remainder are representative values from the literature. CO_2CPU, CO_2 compression and purification unit; EBFGT, Electro beam flue gas treatment.

The technologies that have been reported for simultaneous NO_x and SO_x control are categorized as dry, semi-dry, and wet processes. Dry processes carry out the chemistry on a solid sorbent, catalyst, or with a dry plasma, and yield a dry byproduct, which avoids the need for additional wastewater processing facilities. The Bergbau-Forschung GmbH along with its counterparts developed a multi-pollutant removal technology for heavy metals, dioxins, SO_2 and NO_x by using activated coke as both adsorbent and catalyst[60], for which several of the processes have been developed on a commercial scale. The process is carried out in a moving bed at temperatures between 100°–170°C, wherein high absorption levels are obtained for both SO_2 and NO_x. However, the regeneration process requires a high temperature (400°C) to obtain satisfactory decomposition of dioxins, as well as large amount of water to achieve high removal of H_2SO_4 from the pores of the activated carbon. Therefore, the process is preferred for use in niche processes, such as sinter plants and metallurgical off-gases, where mercury (Hg) or dioxin needs to be removed simultaneously with SO_2 and NO_x. Mochida et al.[84] have performed a study on activated carbon fibers, employing lower operating temperature at 40°–100°C and regeneration temperature at 30°C. However, it is shown that the desulfurization performance in this set-up is inhibited by the presence of NO, hence further study is required to improve the process. Regeneration processes are a common bottleneck among the dry processes, which also hinders the development of simultaneous removal using metal-oxide sorbent[64] and alkali sorbent[65], as they carry significant amount of energy demand. Furthermore, dry processes offer valuable byproducts that can generate additional revenue rather than additional waste management costs. However, the recovered byproduct brings value only when local offtake is available, as in the case of the combined catalytic process, known as DESONOx[62]. The use of a multiple catalyst implies a higher operational cost, so economic viability depends heavily on the market for sulfuric acid. While high-energy electron beam and plasma routes can yield fertilizer byproducts, they are energy-intensive and difficult to scale[68, 70, 71].

Semi-dry processes to remove SO_x and NO_x are developed based on a commercial technology used for desulfurization. Oxidizing agent for NO is added to obtain NO_2, which inherently reacts with a spray of aqueous desulfurizing reagent that is flash-dried, resulting in dry salts of sulfate and nitrate. Despite the proven high removal of SO_2, the process gives considerably low levels of NO_x removal[72-75].

Finally, the wet processes are defined as removal technologies which absorb the pollutants in the aqueous phase. The processes range from gas-phase ozone oxidation feeding a wet scrubber (commercialized by Linde as LoTOx)[76, 77], through oxidant-enhanced wet FGD, and

sulfite/alkali co-absorption, to ammonia scrubbing, and pressurized oxidative absorption [19, 78, 80]. The distinction between oxidative wet scrubbing processes relates to the phase of oxidizing agent that determines where the oxidation of NO occurs, and whether it constitutes a separate unit operation. For a gas-phase oxidant, NO is oxidized in a dedicated reactor or duct upstream of the absorber. Oxidation and absorption are physically and chemically distinct steps, and the absorber can treat a gas flow enriched in NO_2 or N_2O_5. In processes that use a liquid oxidizing agent, the oxidant is dissolved in the scrubbing liquid itself, so that the NO is oxidized and absorbed simultaneously in the liquid phase within a single vessel. Each configuration entails distinct implications in terms of reactor numbers, oxidant handling and utilization, residence-time requirements, byproduct chemistry, and NO removal performance. Both arrangements normally operate at near-atmospheric pressure, while processes that operate at higher pressures represent a new route of NO oxidation. The following section discusses each oxidation route and summarizes the relevant processes.

2.4.1 Gas-phase oxidation

In two-stage processes, the oxidizing agent is introduced into a reactor or duct upstream of the wet absorber. Therefore, the chemistry of NO conversion can be tuned independently of the absorption chemistry, and an existing scrubber can be retrofitted simply by modifying the process so as to be preceded by an oxidation stage. The important considerations in this process are the efficiency of the oxidizing agent and the identity of the NO_x delivered to the absorber, which dictate both its solubility and the downstream liquid chemistry. Ozone is the most-thoroughly studied oxidant, for which Zhang et al.[85] established the governing relationship in a laboratory-scale packed-bed system, injecting O_3 upstream of a NaOH scrubber and showing that NO is converted essentially stoichiometrically to NO_2 (one mole of O_3 per mole of NO). It has been shown that the most-effective NO_x scrubbing is obtained at an O_3/NO molar ratio of about 0.6[85]. Driving the O_3/NO ratio above unity results instead in the formation of NO_2, N_2O_5 and HNO_3, which increased the overall NO_x capture but consumes more ozone and shifts the byproduct toward NO_3^-. The same study[85] reported on how the presence of SO_2 enhances NO_x removal, as dissolved SO_2 forms sulfite (SO_3^{2-}), which acts as a reducing absorbent for NO_2.

Scale-up of the process was demonstrated, for which the O_3/NO_x molar ratio remained the single controlling variable for NO_x removal efficiency, and a higher inlet NO_x concentration increased the rate of absorption at modest cost[76]. This previous work underpins the commercial LoTOx process (Linde Gas AB, Solna, Sweden)[77], the principal attraction of which is that the

ozone pre-oxidation stage can be retrofitted ahead of an existing limestone–gypsum or caustic scrubber. The most-relevant aspect of the process is its cost for electricity to generate ozone on-site, which scales directly with NO_x load and makes the route most attractive for the removal of moderate levels of NO_x, rather than high-NO_x coal boilers[77].

The high cost associated with ozone and the risk of ozone slip have motivated the search for an oxidant that can oxidize NO selectively, that is without any impact on SO_2. Previous work in our research group has proposed gaseous chlorine dioxide (ClO_2) as an alternative, with the gas-phase chemistry revealing that ClO_2 oxidizes NO efficiently at temperatures above 100°–180°C, while having negligible reactions with SO_2[86]. This selectivity profile is highly favorable in terms of the process economics, as the oxidants are consumed almost entirely by the target pollutant. The concept has been applied at three scales (0.2, 100 and 400 Nm^3/h)[80] to flue gases with different origins, confirming selective NO oxidation at all scales and showing consistent NO_x-removal trends, while demonstrating that the smallest reactor gave the highest absolute level of NO_2 absorption owing to more-favorable gas–liquid contacts. The scale-up experiments establish the knowledge gap addressed in this thesis, as S(IV) is found to be oxidized rapidly in the absorber, at a rate that is much faster than the available reaction kinetics.

Apart from ozone and ClO_2, other gas-phase oxidants are confined to narrower windows. Collins et al.[87] performed hot-gas injection of hydrogen peroxide which converts >90% of NO at around 500°C, although it is ineffective at the lower temperatures of a conditioned flue gas because H_2O_2 decomposes too slowly to generate oxidizing radicals. To overcome this temperature constraint, Zhao et al.[88] introduced a vaporized enhanced-Fenton reagent consisting of H_2O_2, FeO_4, and peroxyacetic acid (PAA) into the gas stream and demonstrated that gas-phase Fenton chemistry can oxidize NO with acceptable residence times at 60—120°C. Hao et al.[89] then showed that adding UV irradiation to vaporized H_2O_2 markedly accelerated NO oxidation, establishing photo-activation as a route to low-temperature peroxide oxidation. In-duct generation of •OH radicals from O_2^+ ions and water vapor offer a reagent-free alternative, although this approach remains at an early experimental stage[90].

Table 5 *Gas oxidizing agents for simultaneous NO_x-SO_x removal.*

Method / oxidant	Configuration	Key finding	Ref.
Ozone (O_3) + NaOH	O_3 injected upstream, then packed-bed NaOH scrubbing	Max NOx removal at O_3/NO ≈ 0.6	[85]
Ozone (O_3) + limestone–gypsum	Separate O_3 reactor + limestone–gypsum scrubber	First industrial scale (26,000 SCFM)	[77]
Chlorine dioxide, $ClO_{2(g)}$	$ClO_{2(g)}$ oxidation upstream + alkaline absorption	ClO_2 highly selective to NO; S(IV) rapidly oxidized	[80, 86]
H_2O_2	H_2O_2 injected into hot flue gas, then scrubber	> 90% NO at ≈ 500°C	[87]
Vaporized enhanced-Fenton	Oxidation with fenton reagent composed of H_2O_2, $FeSO_4$, and peroxyacetic acid (PAA) and absorption with $Ca(OH)_2$	>80% NO oxidation between 60—120°C, minimal interaction between oxidant and SO_2	[88]
Vaporized H_2O_2 + UV	Vapor-phase H_2O_2 + UV	UV strongly accelerates the gas-phase reaction	[89]
•OH radicals (O_2^+/ H_2O vapor)	In-duct radical generation	Novel gas-phase radical-driven oxidation	[90]

The principal advantages of the gas-phase oxidation method are that the oxidation stage can be designed, dosed and optimized independently of the scrubber, and that an existing FGD absorber can frequently be retained and simply preceded by an oxidation reactor. The penalties are linked to the need for an additional unit operation and the corrosion-resistant materials required to handle these reactive oxidants, which together increase both the capital and maintenance costs. Table 5 summarizes the studies of specific oxidants used for simultaneous NO_x-SO_x removal, their reported performance levels, and the main findings.

2.4.2 Liquid-phase oxidation

In single-stage processes, the oxidant is dissolved in the scrubbing liquid itself, such that NO is oxidized and absorbed within the same vessel and no separate oxidation reactor is required. The method offers a compact process at the cost of limited NO removal, which is now limited by the gas–liquid mass transfer. The foundational demonstration came from Hutson et al.[78], who tested various water-soluble oxidants, of which $KMnO_4$ and $NaClO_2$ shows the most promising result for NO_x removal. The oxidizing salt $NaClO_2$ was then evaluated in a limestone ($CaCO_3$) wet scrubber and achieved complete removal of SO_2 and mercury, near-complete oxidation of NO, and 60% capture of the resulting NO_x as NO_2 in a single bench-scale vessel. The results also showed that in the absence of SO_2, NO oxidation declined dramatically to roughly 50%. This established the potential of chlorite while revealing the main issue of

unsatisfactory NO_x capture, which led to a subsequent study by Wang et al.[91] on how to combine chlorite with a second oxidant or a stronger absorbent. The $NaClO_2/CaO_2$ oxidant–absorbent, in which CaO_2 supplies both additional oxidizing capacity and alkalinity, increase the NO and NO_x removal levels to 99.4% and 95.0%, respectively, alongside 98%–99.9% SO_2 removal. Hao et al.[92] formulated an $NaClO_2/Na_2S_2O_8$ complex oxidant combined with sodium-humate absorbent, which gave SO_2 and NO absorption of 100% and 82.7%, respectively. They identify the synergistic effect of $NaClO_2$ and $Na_2S_2O_8$ which contribute to the increase of NO_x absorption.

Furthermore, Jin et al.[93] studied ClO_2 directly by generating ClO_2 in situ using the chlorate–chloride process and feeding it into a laboratory-scale bubbling reactor. They obtained complete oxidation of NO to NO_2 once sufficient ClO_2 had been supplied, reaching ~100% SO_2 and 66%–72% NO_x removal at 45°C. Their study exposed the defining constraint of all chlorine-based, single-stage systems as being the low pH level at which ClO_2 oxidizes NO efficiently, whereas NO_2 is absorbed efficiently only at high pH levels.

The drawbacks of chlorine reagents motivated a shift toward radical-based oxidants generated in situ. Persulfate ($S_2O_8^{2-}$) attracted attention because it can be activated in several ways within the liquid. Adewuyi et al.[94] tested the thermal/Fe^{2+} co-activation which sharply increased NO

Table 6 *Liquid oxidizing agents for simultaneous NO_x and SO_x removal.*

Method / oxidant	Configuration	Key finding	Ref.
$NaClO_2$	Oxidant dissolved in $CaCO_3$ scrubbing liquid	SO_2, NO_x and Hg removed simultaneously; SO_2 presence is key for high removal of other pollutants	78
$NaClO_2$ / CaO_2	Combined oxidant–absorbent	High absorption level: SO_2, 98%–99.9%; NO, 99.4%; NO_x, 95%	91
$NaClO_2$ / $Na_2S_2O_8$	Complex oxidant in absorbent + sodium-humate absorbent	Optimal 1 wt% : 1 wt% ratio; $Na_2S_2O_8$ reaction mechanism	92
Aqueous ClO_2	ClO_2 dissolved in potassium iodide scrubbing solution	Lower NO_x removal at higher pH due to less efficient oxidation	93
Heat + Fe^{2+} persulfate	Activated persulfate absorbent	Heat activation with and without Fe^{2+} offer similar removal levels; highly temperature dependent	94
UV + heat $(NH_4)_2S_2O_8$	UV-activated persulfate absorbent	UV yields far more radicals than heat alone	95
$KMnO_4$	Permanganate absorbent	Direct NO → nitrate; MnO_2 fouling	78, 79, 96

removal from 46% to 79% as the temperature rose from 30°C to 70°C, with SO_2 and Fe^{2+} each independently promoting removal by accelerating radical generation. Building on this, the work of Liu et al.[95] evaluate a UV/thermal co-activation of ammonium persulfate, achieving 96.1% NO removal and 100% SO_2 removal. They reported that UV produced far more radicals than heat alone, thereby confirming that radical density sets the removal rate. Aside from these radical systems, a range of studies[78, 79, 96] investigated potassium permanganate ($KMnO_4$) which is also a strong oxidant for NO by directly oxidizing NO to nitrate via a Mn(VII)→Mn(IV) two-electron step. It removes 45% of the NO because the reaction is too slow to compete with the short gas–liquid contact time, and the MnO_2 precipitate and fouls the packing, nozzles, and pumps which can itself suppress SO_2 uptake.

The appeal of the liquid oxidation process is that it entails a single, compact device with no separate oxidation reactor and straightforward integration of oxidant dosing into the absorbing liquid. Its characteristic limitation is that NO removal is governed by the gas–liquid mass transfer of an insoluble gas, which means that performance depends strongly on the interfacial area and contact time. While SO_2 removal is straightforward regardless of the oxidant, NO_x removal is constrained by the competition between the rate of liquid-phase NO oxidation and the mass transfer of a poorly soluble gas. Table 6 summarizes the various liquid-phase oxidizing agent and their corresponding performance levels.

2.4.3 Pressurized absorption

A distinct method for oxidizing NO is the pressurized system, in which NO oxidation is enabled by the high partial pressure rather than added chemicals. The rate of the third-order, gas-phase oxidation increases steeply with increasing pressure, so that at 10–30 bar NO is converted to NO_2 rapidly using only the oxygen present in the flue gas.

The principal industrial embodiment of this method is the “sour compression” process, developed for oxy-fuel combustion carbon capture, in which the CO_2-rich flue gas is already compressed for storage and NO_x and SO_x are co-removed during the compression stage. Air Products (Air Products and Chemicals Inc., Allentown, PA, USA) and Vatttenfall[83] performed a demonstration of a two-stage high-pressure scrubbing system using a slipstream from Vattenfall’s 30 MWth oxyfuel pilot plant. The results showed that SO_2 is almost completely removed after the first stage of compression (15 bar), along with 80% of the NO_x. White et al.[97] performed a pilot-scale investigation using the side stream of Doosan Babcock 160-kW coal-fired oxyfuel rig. A one-stage compression process at various pressure was performed, in

which 84% of SO_2 removal and 68% of NO_x removal was achieved at 7 bar, with increasing removal levels obtained at 14 bar.

Studies on the nitrogen-sulfur chemistry have confirmed that the NO to NO_2 conversion governs the overall NO_x removal and is strongly promoted by pressure increases[97], while suppressed by SO_2 concentration increases[98]. Cheng et al.[99] performed detailed product analysis in a high-pressure bubbling column and identified hydroxylamine disulfonic acid (HADS) as the dominant liquid product at pH levels ≥ 4, while N_2O is formed between a pH of 1—4. Practical limitations occur as SO_2 can revert part of the NO_2 back to NO, thereby decreasing the level of NO_x removal. Studies conducted to date on pressurized absorption systems are summarized in Table 7.

Table 7 *Pressurized oxidative-absorption studies: NO oxidized to NO_2 by the flue gas's own O_2 under pressure, with simultaneous absorption of NO_2 and SO_2.*

System / study	Pressure	Key finding / mechanism	Ref.
Air Products two-stage high-pressure scrubbing	15 bar (stage 1) and 30 bar (stage 2)	Foundational sour-compression concept	83
Doosan Babcock 160-kW oxyfuel pilot	3–14 bar	Establish the effect of pressure to NO_x and SO_2 removal	97
Oxy-fuel CO_2-compression denitrification	up to 20 bar	NO oxidation rises with pressure increase, falls with T temperature increase; increasing SO_2 concentration lowers NO_x removal	98
High-pressure bubbling column (CO_2CPU)	High pressure	HADS found as main product; acids corrode 316L stainless steel	99

CO_2CPU, CO_2 compression-and-purification unit; HADS, hydroxylamine disulfonic acid.

3 Chemistry

This thesis focuses on the absorption stage following a gas-phase oxidation process, such that no oxidant is present in the system and NO_2 is considered as the sole oxidation product. This chapter presents the chemistry involved in a system with N_2, O_2, NO_2, SO_2, and CO_2 in the gaseous phase. The aqueous-phase consists primarily of water, in which various ions are present as a result of gas dissolution or the addition of salts. The reactions described in the following section apply to a liquid pH level >5, based on the Chalmers Acidic Nitrogen and Sulfur (ChAINS) mechanism[100]. An overview of the reaction scheme is provided in Figure 3.

Gas phase chemistry

At atmospheric pressure, the gaseous phase reactions play less-significant roles in the absorption process, as compared with a pressurized system. The gaseous reactions considered in this study are the oxidation of NO to NO_2 based on R_g1:

$$2NO + O_2 \leftrightarrow 2NO_2 \qquad (R_g1)$$

and the dissociation of HNO_2 according to R_g2:

$$HNO_2 \leftrightarrow NO_2 + NO + H_2O \qquad (R_g2)$$

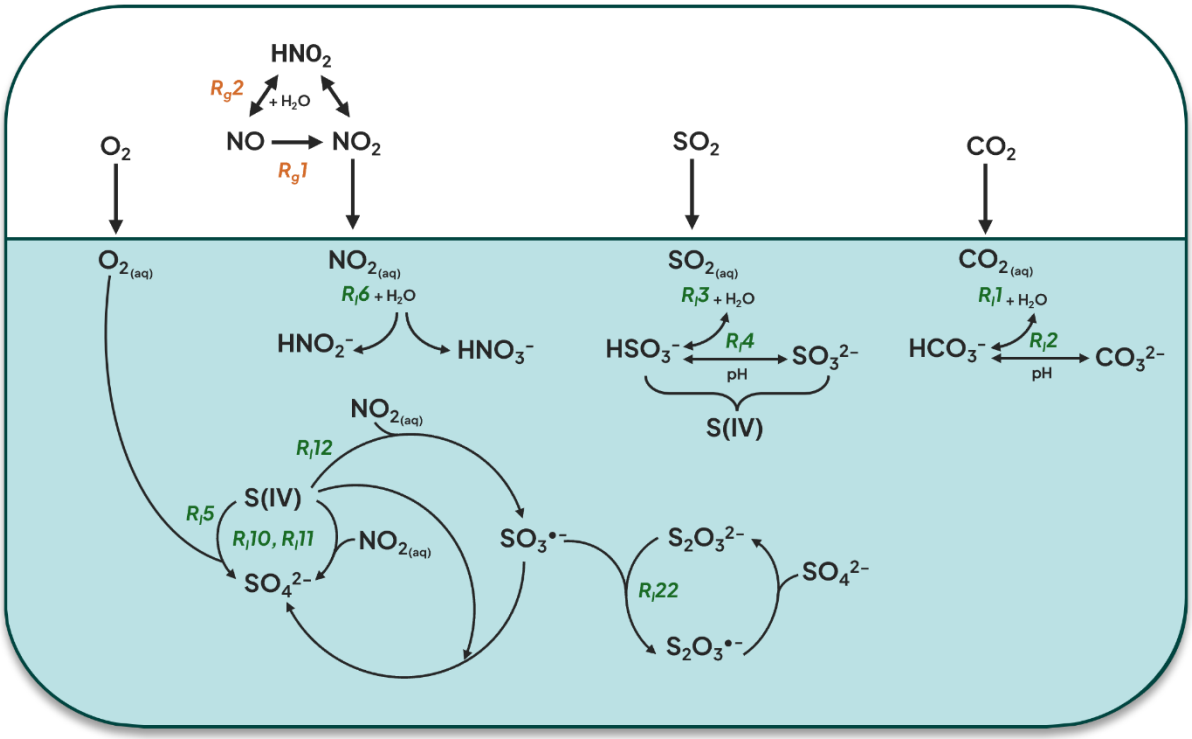

Figure 3 *Overall reaction mechanism for the gas-liquid system. The gas phase is represented in white and the aqueous phase in green. Reaction labels are denoted in yellow.*

Liquid phase chemistry

In the liquid phase, CO_2 dissolves in water to form H_2CO_3, which dissociates into H_+ and HCO_3^- where the net reaction occurs according to R_l1:

$$CO_{2(aq)} + H_2O_{(l)} \leftrightarrow H^+ + HCO_3^- \quad (R_l1)$$

HCO_3^- increasingly dominates as the liquid pH increases beyond 6.35[101]. As the pH increases further to approach 10.33, HCO_3^- dissociates further to form CO_3^{2-} through R_l2:

$$HCO_3^- \leftrightarrow H^+ + CO_3^- \quad (R_l2)$$

The dissolution of SO_2 is the key reaction that generates sulfur ions in the liquid phase. SO_2 readily reacts with water to form S(IV) ions through R_l3:

$$SO_{2(aq)} + H_2O_{(l)} \leftrightarrow H^+ + HSO_3^- \quad (R_l3)$$

In the aqueous phase, HSO_3^- is in equilibrium with SO_3^{2-} based on the instantaneous reaction R_l4:

$$HSO_3^- \leftrightarrow H^+ + SO_3^{2-} \quad (R_l4)$$

The distribution of S(IV) species is pH-determined, with HSO_3^- as the dominant species up to pH 6, while further increase in pH corresponds with an increase in the concentration of SO_3^{2-} ions. In the presence of oxygen, SO_3^{2-} is oxidized to SO_4^{2-} according to R_l5:

$$2SO_3^{2-} + O_{2(aq)} \rightarrow 2SO_4^{2-} \quad (R_l5)$$

Upon dissolving in water, NO_2 reacts according to R_l6:[100]

$$2NO_{2\ (aq)} + H_2O_{(l)} \rightarrow HNO_{2\ (aq)} + HNO_{3\ (aq)} \quad (R_l6)$$

HNO_2 can then dissociate to form NO and NO_2 through R_l7. Both nitrous acid and nitric acid will instantaneously dissociate according to R_l8 and R_l9:

$$HNO_{2\ (aq)} \leftrightarrow NO_2 + NO + H_2O \quad (R_l7)$$

$$HNO_{2\ (aq)} \leftrightarrow H^+ + NO_2^- \quad (R_l8)$$

$$HNO_{3\ (aq)} \leftrightarrow H^+ + NO_3^- \quad (R_l9)$$

The interaction between S(IV) and NO_2 is an important aspect, as the NO_2 absorption level has been shown to be dependent upon the concentration of S(IV)[23]. Clifton et al.[29] have proposed that the overall reaction between NO_2 and S(IV) in this system to correspond to R_l10 and R_l11:

$$2NO_{2\ (aq)} + SO_3^{2-} + H_2O_{(l)} \rightarrow 2NO_2^- + SO_4^{2-} + 2H^+ \quad (R_l10)$$

$$2NO_{2\ (aq)} + HSO_3^- + H_2O_{(l)} \rightarrow 2NO_2^- + SO_4^{2-} + 3H^+ \quad (R_l11)$$

The rate of S(IV) depletion has been shown to be more rapid than the concurrent absorption of NO_2. The oxidation rate is also significantly faster than the sole oxidation of S(IV) by oxygen

(R_I5), in addition to being more rapid than the proposed rates for R_I10 and R_I11. Littlejohn et al.[25] have proposed the following radical chain reaction mechanism:

$$NO_{2\,(aq)} + SO_3^{2-} \rightarrow NO_2^- + 2SO_3^{\bullet-} \quad (R_I12)$$

$$SO_3^{\bullet-} + SO_3^{\bullet-} \rightarrow S_2O_6^{2-} \quad (R_I13)$$

$$SO_3^{\bullet-} + SO_3^{\bullet-} \rightarrow SO_3^{2-} + SO_3 \quad (R_I14)$$

$$SO_3 + H_2O \rightarrow 2H^+ + SO_4^{2-} \quad (R_I15)$$

$$SO_3^{\bullet-} + O_2 \rightarrow SO_5^{\bullet-} \quad (R_I16)$$

$$SO_5^{\bullet-} + SO_3^{2-} \rightarrow SO_5^{2-} + SO_3^{\bullet-} \quad (R_I17)$$

$$SO_5^{\bullet-} + SO_3^{2-} \rightarrow SO_4^{2-} + SO_4^{\bullet-} \quad (R_I18)$$

$$SO_4^{\bullet-} + SO_3^{2-} \rightarrow SO_4^{2-} + SO_3^{\bullet-} \quad (R_I19)$$

$$SO_5^{2-} + H^+ \leftrightarrow HSO_5^- \quad (R_I20)$$

$$HSO_5^- + SO_3^{2-} \rightarrow SO_4^{2-} + SO_4^{2-} \quad (R_I21)$$

R_I12 to R_I15 are proposed to reflect the reaction mechanism in the absence of O_2, as more $S_2O_6^-$ is found in the product. As O_2 is added to the system, the proportion of SO_4^{2-} increases and the complete series of reactions (R_I12 to R_I21) is suggested to take place.

An oxidation inhibitor, namely thiosulfate $S_2O_3^{2-}$, can be added to the system. Mo et al. [102] have outlined the mechanism for thiosulfate inhibition as:

$$R^{\bullet} + S_2O_3^{2-} \rightarrow R + S_2O_3^{\bullet-} \quad (R_I22)$$

$$R^{\bullet} + S_2O_3^{\bullet-} \rightarrow Polythionate \quad (R_I23)$$

$$S_2O_3^{\bullet-} + S_2O_3^{\bullet-} \rightarrow Polythionate \quad (R_I24)$$

$$Polythionate + H_2O \rightarrow S_2O_3^{2-} + SO_4^{2-} + 2H^+ \quad (R_I25)$$

Reactions R_I22 and R_I23 will scavenge the radical species, breaking the radical chain reaction that starts with R_I12. The radical chain is terminated through R_I24, which significantly reduces sulfite consumption.

4 Methods

In this thesis, the rapid oxidation of S(IV) is investigated by addressing the difference between the observed and calculated S(IV) consumption levels. As illustrated in Figure 4, the work in **Paper I** uses kinetic modeling to obtain kinetic expressions for the proposed mechanism. These findings are thereafter incorporated into the process modeling software in **Paper II**, such that the kinetic parameters are further refined to model the relevant industrial process.

4.1 Kinetic model development

The kinetic model is designed to resolve the issues of rapid depletion of S(IV) ions and radical scavenging by thiosulfate, as observed in the laboratory-scale experimental work in our research group[103] (described in greater detail in **Paper I**). The chemistry of the system becomes increasingly complex with the addition of new species. This is due to their individual reactions, the effect of mass transfer, and the interactions that occur between different species in the system. To distinguish these effects, the model is developed by initially modeling the key reactions in isolation, before gradually introducing more species into the system, as illustrated in Figure 5.

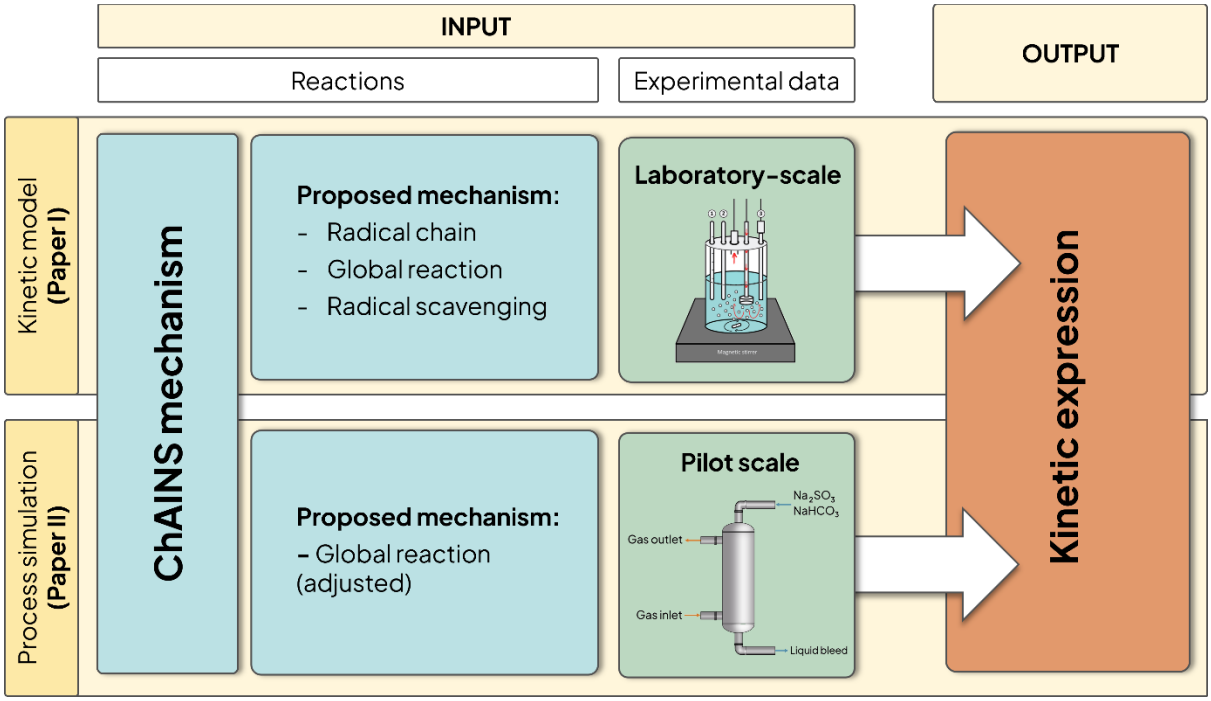

Figure 4 *Overview of the modeling approaches used in this thesis, their main data inputs, and target outputs. ChAINs: Chalmers Acidic Nitrogen and Sulfur mechanism.*[100]

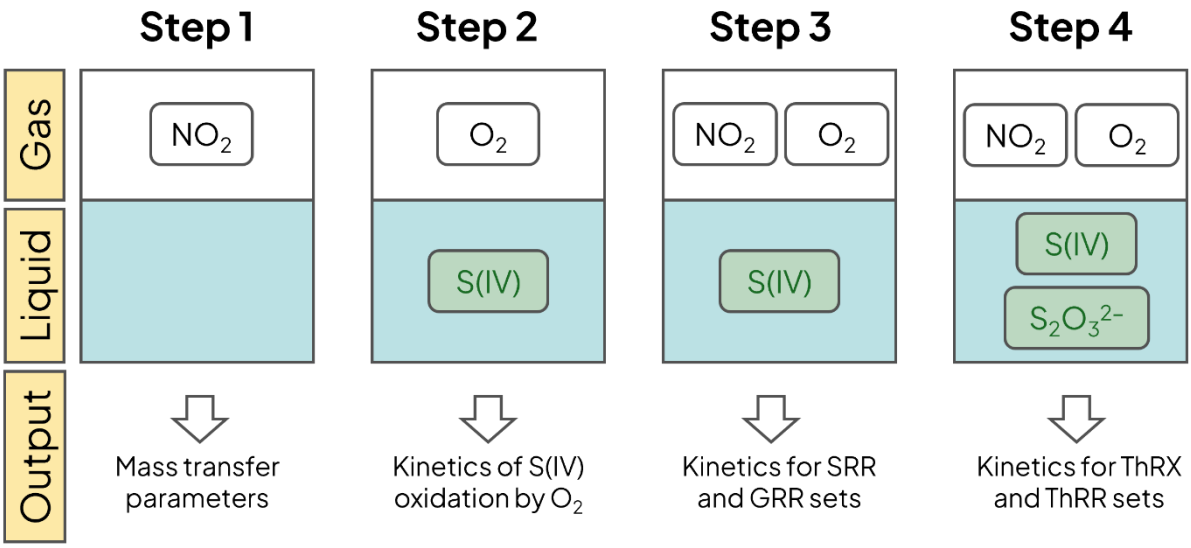

Figure 5 *Stepwise development of the reactor models.*

Steps 1 and 2: Mass transfer model and reference mechanism calibration

The initial steps are modeled using the ChAINS mechanism[100], involving a reduced mechanism for pH 5 that provides a comprehensive base mechanism for the alkaline condition evaluated in the current work. In Step 1, a system that contains only NO_2 and water is first simulated to evaluate the effects of mass transfer parameters. Different average bubble diameters are tested to identify a range that approximates the observed NO_2 absorption in water.

Step 2 involves observations of the oxidation of S(IV) by O_2. Establishing the rate constant becomes a crucial step, as the reaction contributes to the overall S(IV) consumption. As the rate constant for the reaction varies in the literature, a comparison of the modeling and experimental measurements is used to estimate a suitable kinetic coefficient.

Step 3: Kinetic estimation of NO_2-induced S(IV) oxidation

Gaseous NO_2 is introduced in Step 3, whereby two new reaction sets are proposed to represent the rapid consumption of S(IV). Each of the reaction sets is evaluated separately alongside the reference mechanism. The Sulfite Radical Chain Reaction (SRR) set is formulated by combining the radical chain mechanism suggested by Littlejohn et al.[25] and the qualitative observations made in the laboratory-scale experimental work. The reactions are applied in Step 3, to model the radical species $SO_3^{\bullet-}$ generated through the interaction between $NO_{2(aq)}$ and SO_3^{2-} ($R_{SRR}1$). This leads to the propagation cycle, where $SO_3^{\bullet-}$ reacts with dissolved O_2 to form $SO_5^{\bullet-}$ ($R_{SRR}2$), which subsequently reacts with SO_3^{2-} to produce sulfate while regenerating $SO_3^{\bullet-}$ ($R_{SRR}3$).

$$NO_{2\ (aq)} + SO_3^{2-} \rightarrow NO_2^- + SO_3^{\bullet-} \quad R_{SRR}1$$

$$SO_3^{\bullet-} + O_2 \rightarrow SO_5^{\bullet-} \quad R_{SRR}2$$

$$SO_5^{\bullet-} + 2SO_3^{2-} \rightarrow 2SO_4^{2-} + SO_3^{\bullet-} \quad R_{SRR}3$$

$$SO_3^{\bullet-} + SO_5^{\bullet-} + H_2O \rightarrow SO_4^{2-} + SO_5^{2-} + 2H^+ \quad R_{SRR}4$$

The second reaction set proposed for the NO_2-induced S(IV) oxidation is the Global Radical Reaction (GRR) set, which is developed to represent the net effect of radical propagation while excluding the short-lived intermediates. Instead of a sequence of radical reactions, a higher stoichiometric coefficient is applied for SO_3^{2-} to capture the rapid consumption.

$$2NO_{2\ (aq)} + 7SO_3^{2-} + H_2O + 3O_2 \rightarrow 2NO_2^- + 7SO_4^{2-} + 2H^+ \quad R_{GRR}$$

Step 4: Kinetic estimation of radical scavenging by thiosulfate

In the last step, $S_2O_3^{2-}$ is introduced to the aqueous phase and the two radical scavenging mechanisms are proposed, with the sulfite radical chain reaction as the basis. The Thiosulfate Regeneration Reaction (ThRX) set is based on the mechanism reported by Mo et al.[102], in which thiosulfate reacts with $SO_3^{\bullet-}$, effectively interrupting the radical propagation chain, which leads to a lower level of S(IV) consumption. Polythionates ($S_4O_6^{2-}$) are present in the mechanism as intermediates, which further react to form sulfate and regenerate $S_2O_3^{2-}$.

$$SO_3^{\bullet-} + S_2O_3^{2-} \rightarrow SO_3^{2-} + S_2O_3^{\bullet-} \quad R_{ThRX}1$$

$$S_2O_3^{\bullet-} + S_2O_3^{\bullet-} \rightarrow S_4O_6^{2-} \quad R_{ThRX}2$$

$$S_4O_6^{2-} + SO_3^{2-} \rightarrow SO_4^{2-} + S_2O_3^{2-} + SO_2 \quad R_{ThRX}3$$

Since the presence of polythionates is not observed in the experimental work, a second radical scavenging pathway is proposed. The simplified Thiosulfate Radical Chain Reaction (ThRR) set entails more-condensed steps without the formation of $S_4O_6^{2-}$.

$$SO_3^{\bullet-} + S_2O_3^{2-} \rightarrow SO_3^{2-} + S_2O_3^{\bullet-} \quad R_{ThRR}1$$

$$2S_2O_3^{\bullet-} + 2O_2 \rightarrow SO_4^{2-} + 3SO_2 \quad R_{ThRR}2$$

4.2 Process simulation

In the process simulation, a new reaction is added to improve predictions of process performance and to identify the important operating conditions. A modified version of R_{GRR}, termed $R_{N\text{-}S}$, is applied in the process modeling to capture the S(IV) consumption observed in the column:

$$2NO_{2\,(aq)} + 100SO_3^{2-} + H_2O_{(l)} + 49.5O_2 \rightarrow 2NO_2^- + 100SO_4^{2-} + 2H^+ \qquad R_{N\text{-}S}$$

The stoichiometric coefficient of SO_3^{2-} is significantly higher compared to R_{GRR}, which is intended to achieve a balanced correlation between the level of absorbed NO_2 and oxidized S(IV).

The two process configurations investigated in this thesis are illustrated in Figure 6. The open-loop simulation is used to evaluate the global reaction proposed in **Paper I** and to modify it accordingly. Updated kinetic parameters are obtained by comparing the modeling results to the experimental data obtained from a pilot-scale packed column, as described in **Paper II**. The evaluated gas flow contains CO_2, O_2, N_2, and traces of NO_2, which are injected from gas bottles at the desired inlet concentrations. Furthermore, a solution containing Na_2SO_3 at varying concentrations and $NaHCO_3$ enters at the top of the column. Using Fourier Transform Infrared (FTIR) spectroscopy, the gas compositions in the inlet and outlet flows are measured, while samples from the liquid inlet and outlet are analyzed in a chemistry laboratory using titration.

Following the global reaction adjustment in the open-loop model, the proposed reaction is evaluated in a closed-loop configuration that is based on a 400 Nm^3/h test unit[23] in a waste incineration plant. The flue gas contains CO_2, O_2, N_2, SO_2, and NO_2 at concentrations that vary according to the fuel composition and operating conditions. For the purpose of the present work, a single measurement point is used to ensure a valid comparison of the model and the measurement. A makeup flow of water, NaOH, and Na_2SO_3 are supplied to maintain the desired liquid-to-gas (L/G) flow ratio and inlet pH level.

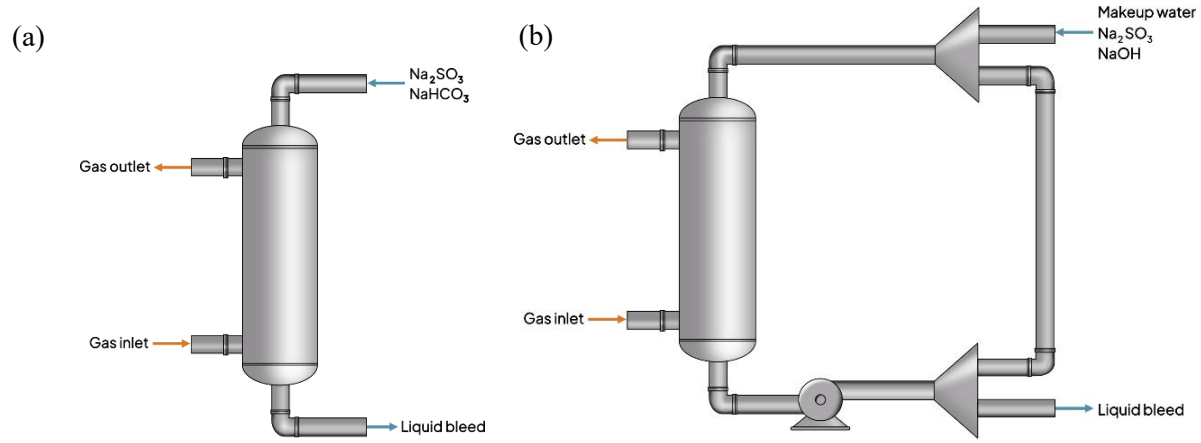

Figure 6 *Aspen Plus process scheme for the: (a) open-loop configuration; and (b) closed-loop configuration.*

The process performance is evaluated based on the levels of NO_2 absorption and S(IV) oxidation, as defined by Equations (1) and (2), respectively.

$$NO_2\ absorption = \frac{F_{NO_2\ in} - F_{NO_2\ out}}{F_{NO_2\ in}} \quad (1)$$

$$S(IV) oxidation = \frac{F_{S(IV)\ in} - F_{S(IV)\ out}}{F_{S(IV)\ in}} \quad (2)$$

where F is the mole flow (in kmol/h) and the S(IV) ions include SO_3^{2-}, HSO_3^-, and $SO_{2(g)}$.

In addition, a sensitivity analysis is performed to identify the effects of varying the operating conditions. A normalized sensitivity factor[104] (S) [Equation (3)] is used to quantify the relative changes in process performance (Y) as alterations are made to the operating conditions (X).

$$S = \frac{\frac{|\Delta Y|}{Y_{ref}}}{\frac{|\Delta X|}{X_{ref}}} \quad (3)$$

5 Results and discussion

5.1 Kinetics and mechanism of S(IV) oxidation

5.1.1 Parameter estimation for S(IV) oxidation by O_2

Following the mass transfer calibration, the kinetic coefficient for S(IV) oxidation by O_2 (R_l5) is obtained by fitting the calculated S(IV) concentration to experimental data, using the suggested kinetics of Beilke et al.[28] in which the concentration of H^+ ions is included in the rate expression. The obtained k_{R_l5} is presented and compared to reported values of pseudo-first-order rate coefficient in the literature in Table 8. The kinetics obtained in this work is lower than most of the reported values. Note that the pH level may influence the reaction rate. The S(IV) consumption rate in the experiment has the same magnitude as those of the mannitol-inhibited system, although no inhibiting species is expected to be present in the setup. The lower reaction rate is attributed to differences in experimental set-up, which affect the extent of gas dissolution into the liquid phase. In our experiments, we flushed the system with N_2 at the beginning of the run, thereby starving the system of dissolved O_2 for reaction. Meanwhile, other groups[28, 105, 106] allowed the liquid and gas in the headspace to achieve equilibrium before adding the sulfite solution, leading to a more-effective reaction between the dissolved gas species and sulfite salts.

5.1.2 Modeling results for S(IV) oxidation by NO_2

Proposed reaction mechanism based on laboratory-scale experiments

After establishing the core reactions in the system, gaseous NO_2 was added in the model while applying the ChAINS mechanism[100]. Figure 7 shows the comparison of the modeling results and measured data, where a clear difference in S(IV) consumption is evident. A lower NO_2 outlet concentration is predicted by the model, as more $NO_{2(g)}$ reacts together with the large amount of S(IV) in the system.

Table 8 *Pseudo-first-order kinetic coefficients for S(IV) oxidation by O_2, as obtained in the present work and reported in the literature.*

Reference	Inhibitor	pH	Pseudo-first-order k (s^{-1})
Current work	–	7	$7.9e^{-5*}$
Beilke et al.[28]	–	$3-6$	$1.58e^{-3*}$
Fuller and Crist[105]	Mannitol	–	$1.5e^{-5}$
Brimblecombe and Spedding[107]	–	6	$6e^{-4}$
Schroeter[106]	–	8	$6e^{-4}$
Fuller and Crist[105]	–	$8.2-8.8$	$1.3e^{-2}$

*Achieved by multiplying with an $[H^+]$ of $1e^{-7}$ mol/L

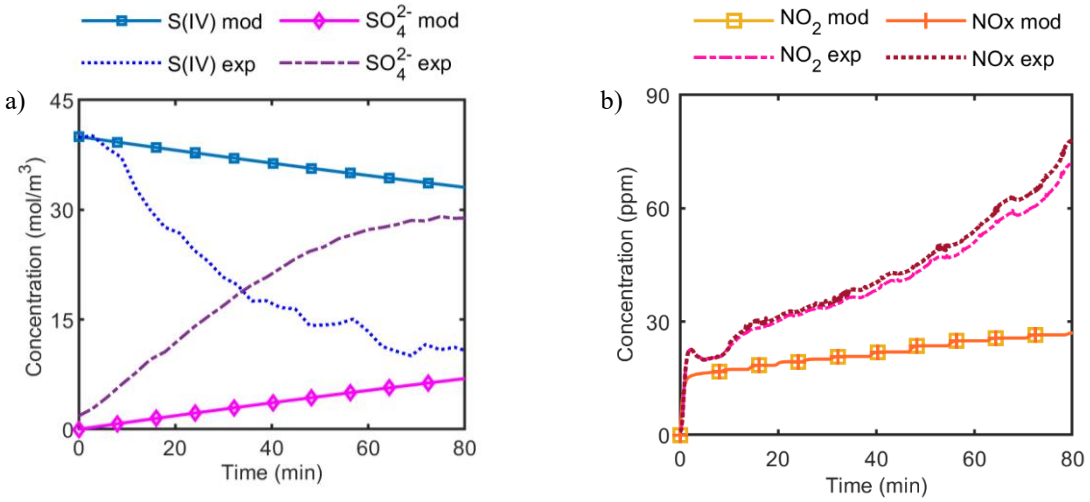

Figure 7 *Liquid (a) and gaseous (b) concentration profiles, estimated with the ChAINS[100] mechanism (solid lines) and laboratory-scale measurements (dotted lines).[103]*

To improve the model, the sulfite radical chain reaction set and the global reaction set were developed. The kinetics obtained for the proposed reactions are summarized in Table 9. In the radical chain reaction, the propagation step ($R_{SRR}2$ and $R_{SRR}3$) drives S(IV) consumption. As shown in Figure 8, the rates of $R_{SRR}2$ and $R_{SRR}3$ are independent of the initiation step ($R_{SRR}1$) because the radical species are maintained in a cycle, which explains how radicals can rapidly deplete S(IV) in the system. The sulfite radical chain reaction shows good agreement with the measured S(IV) concentrations, with a Root Mean Square Deviation (RMSD) of 0.06 (Figure 9a). In comparison, the global reaction has an RMSD of 1.07. The error is mainly due to the lower S(IV) concentration towards the end of the run.

Figure 9b shows the calculated and measured gas outlet concentrations for both the sulfite radical chain and global reaction. The model yields outlet NO_2 concentrations similar to those obtained in the measurements. However, discrepancies are observed in the outlet NO_2 concentration profile over time, which may be attributable to the different approaches used to maintain the pH level. The model assumes that the pH remains at 7, whereas in the experimental series the pH was maintained by titration with NaOH, with minor fluctuations between the additions.

Table 9 *Kinetic rate expressions for the SRR and GRR sets.*

	Reaction	Kinetic rate expression (m^3,mol,s)
RSRR1	$NO_{2\ (aq)} + SO_3^{2-} \rightarrow NO_2^- + SO_3^{\bullet-}$	$r_{SRR_1} = 2\ C_{NO_2} C_{SO_3^{2-}}$
RSRR2	$SO_3^{\bullet-} + O_2 \rightarrow SO_5^{\bullet-}$	$r_{SRR_2} = 2\ C_{SO_3^{\bullet-}} C_{O_2}$
RSRR3	$SO_5^{\bullet-} + 2SO_3^{2-} \rightarrow 2SO_4^{2-} + SO_3^{\bullet-}$	$r_{SRR_3} = 1.9\ C_{SO_5^{\bullet-}} C^2_{SO_3^{2-}}$
RSRR4	$SO_3^{\bullet-} + SO_5^{\bullet-} + H_2O \rightarrow SO_4^{2-} + SO_5^{2-} + 2H^+$	$r_{SRR_4} = 0.2\ C_{SO_3^{\bullet-}} C_{SO_5^{\bullet-}}$
RGRR	$2NO_{2\ (aq)} + 7SO_3^{2-} + H_2O + 3O_2 \rightarrow 2NO_2^- + 7SO_4^{2-} + 2H^+$	$r_{GRR} = 1.24 \times 10^{-4}\ C_{SO_3^{2-}}$

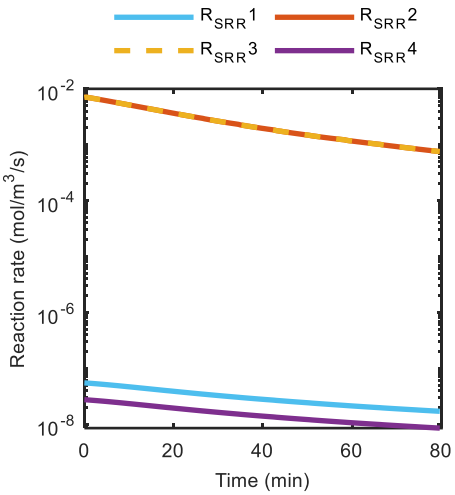

Figure 8 *Rates of reactions 1-4 in the SRR set.*

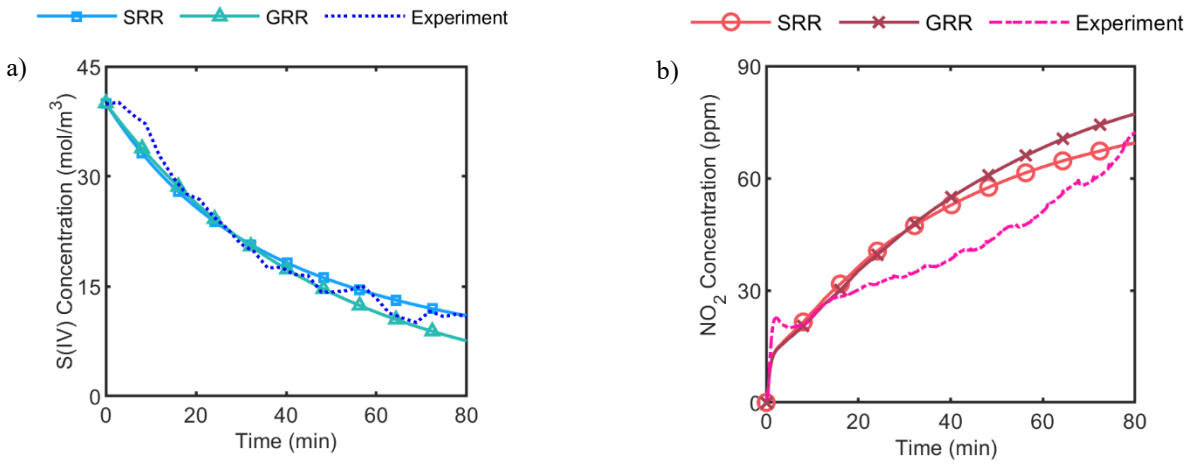

Figure 9 *Liquid (a) and gaseous (b) concentration profiles, estimated by the sulfite radical reaction set (SRR) and the global reaction set (GRR) (solid lines) and measured at laboratory scale (dotted line).*

Process simulation of the global reaction set

The global reaction was integrated into the open-loop model to assess its ability to predict the NO_2 absorption and S(IV) oxidation levels in process units. Initial simulations revealed that fitting both the NO_2 absorption level and S(IV) oxidation level in the absorption column is more challenging compared to the well-stirred reactor. This is due to the low stoichiometric coefficient of SO_3^{2-} used in the global reaction, which represents a substantial correlation between the absorbed NO_2 and oxidized S(IV) levels. To avoid iterating multiple variables, high stoichiometric coefficients were tested and a value of 100 was found to be suitable to accentuate the rapid sulfite oxidation while minimizing its impact on NO_2 absorption. The reaction rate was modified according to the following expression, where the concentration of $NO_{2(aq)}$ was included to account for the more-pronounced concentration gradient in an absorption column:

$$r_{N-S} = k_{R_{N-S}} C_{NO_{2(aq)}} C_{SO_3^{2-}}$$

The kinetic coefficient, $k_{R_{N-S}}$, was estimated using the open-loop model. A rate constant of 9.5e^3 m^3/(mole·s) was calculated. Figure 10 presents a comparison of the S(IV) oxidation and NO_2 absorption levels between the obtained reaction rate and the measurements for the entire set of process configurations tested. The model shows good agreement for cases with high inlet concentrations of S(IV) (Cases 3, 4, 5, and 7), while overestimating S(IV) oxidation for lower inlet concentration. This indicates a proportional relationship between the initial S(IV) concentration and the rate of S(IV) oxidation, as reported previously by Littlejohn et al.[25] and Connick et al.[108].

The proposed reaction was also evaluated in a closed-loop model based on an experiment conducted in a 400 Nm^3/h waste incineration plant test unit, described previously in our group[23]. Table 10 summarizes the results from the experiment and those obtained by simulating different mechanisms. SO_2 absorption is not included in the table as it consistently reaches 99% for all cases. Adding $R_{N\text{-}S}$ to the mechanism results in a slight decrease in NO_2 absorption, despite the high level of S(IV) oxidation, which is evidenced by the significant decrease in the outlet S(IV) concentration. Increasing the $k_{R_{N-S}}$ to 2.5e^4 m^3/(mole·s)yields good agreement for NO_2 absorption, while giving a lower outlet S(IV) concentration than the concentration range suggested by the colorimetric analysis.

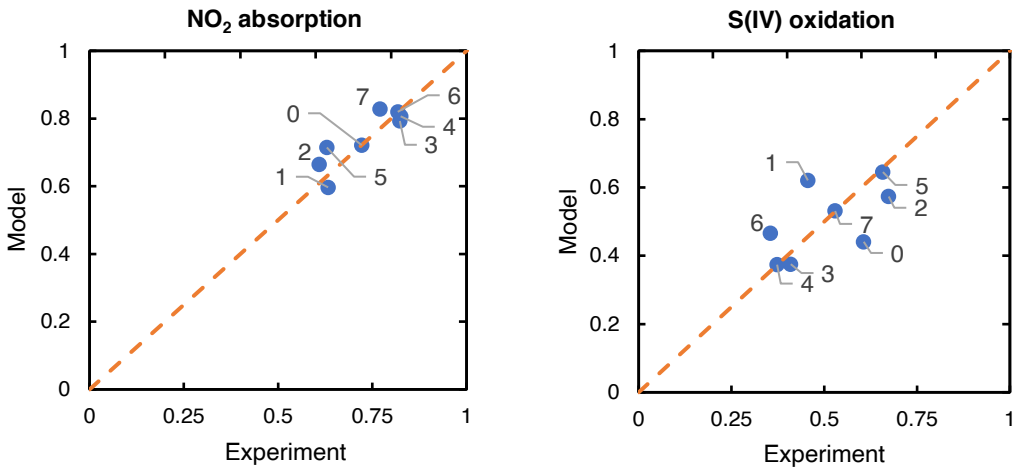

Figure 10 *Comparison of modeling $R_{N\text{-}S}$ reaction and pilot-scale experimental results for NO_2 absorption (left panel) and S(IV) oxidation (right panel).*

Table 10 *Comparison of NO_2 absorption and liquid outlet S(IV) levels. The experimental data for the 400 Nm^3/h case have been reported by Johansson et al.[23].*

	Experimental data	Ajdari et al.[84]	$R_{N\text{-}S}$ (k=9.5e^3)	$R_{N\text{-}S}$(k=2.5e^4)
NO_2 absorption	82%	99.8%	99.5%	82%
S(IV) out (mg/L)	25–50	19,000	4,400	4

5.2 Radical scavenging by thiosulfate

A mechanism for radical scavenging (ThRX) and a simplified reaction set (ThRR), are proposed, as summarized in Table 11. The main difference between the two mechanisms is the presence of polythionates as an intermediate (ThRX) and the involvement of O_2 (ThRR) in the mechanisms. The obtained liquid and gas concentration profiles for both mechanisms are identical, as shown in Figure 11.

A good approximation of the measured S(IV) and sulfate concentrations are obtained, while the measured thiosulfate consumption is not captured by the model. The model reveals that only 0.54 µmol of thiosulfate was consumed by $R_{ThRX}1$ and regenerated thiosulfate was quantified as being as low as 0.27 µmol. Furthermore, the level of polythionates was predicted to approach zero, in agreement with the experimental results, where no polythionates were observed in the final liquid solution. In addition, the minor contribution of thiosulfate regeneration undermines its relevance for the system, confirming the suitability of the simplified reaction set.

Table 11 *Kinetic rate expressions for the radical scavenging reaction sets and simplified reaction sets.*

	Reaction	Kinetic rate expression (m^3,mol,s)
Radical scavenging reaction set		
RThRX1	$SO_3^{\bullet-} + S_2O_3^{2-} \rightarrow SO_3^{2-} + S_2O_3^{\bullet-}$	$r_{ThRX_1} = 113.5\ C_{SO_3^{\bullet-}} C_{S_2O_3^{2-}}$
RThRX2	$S_2O_3^{\bullet-} + S_2O_3^{\bullet-} \rightarrow S_4O_6^{2-}$	$r_{ThRX_2} = 91.62\ C^2_{S_2O_3^{\bullet-}}$
RThRX3	$S_4O_6^{2-} + SO_3^{2-} \rightarrow SO_4^{2-} + S_2O_3^{2-} + SO_2$	$r_{ThRX_3} = 97.68\ C_{S_4O_6^{2-}} C_{SO_3^{2-}}$
Simplified reaction set		
RThRR1	$SO_3^{\bullet-} + S_2O_3^{2-} \rightarrow SO_3^{2-} + S_2O_3^{\bullet-}$	$r_{ThRR_1} = 0.32\ C_{SO_3^{\bullet-}} C_{S_2O_3^{2-}}$
RThRR2	$2S_2O_3^{\bullet-} + 2O_2 \rightarrow SO_4^{2-} + 3SO_2$	$r_{ThRR_2} = 0.99\ C^2_{S_2O_3^{\bullet-}} C^2_{O_2}$

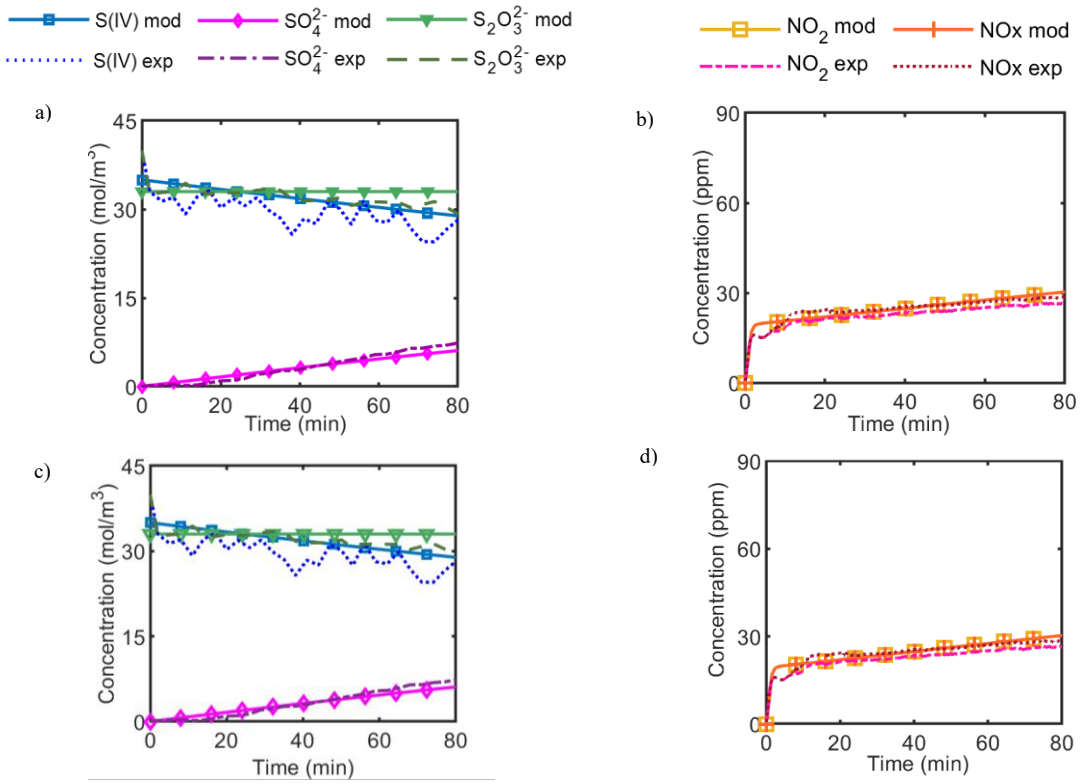

Figure 11 *Concentration profiles of sulfur oxides and nitrogen oxides in the liquid and gaseous phases, respectively, for: (a) and (b), the thiosulfate scavenging mechanism (ThRX); and (c) and (d), the simplified scavenging mechanism (ThRR). mod, Modeled (solid lines); exp, Experimental (dotted lines).*

5.3 Identification of key operating parameters

A sensitivity analysis was performed for the open-loop simulation with the addition of $R_{N\text{-}S}$. The reference condition and varied parameters are described in greater detail in **Paper II.** The effects of the different parameters were normalized to evaluate their net impacts on the process performance indicators, as presented in Figure 12. Parameters relevant to mass transfer, such as interfacial area factors, packed height, and liquid flow rate, demonstrate stronger influences on NO_2 absorption, compared to the reactant inlet concentration. In particular, packed height specifically shows a prominent effect on both NO_2 absorption and S(IV) oxidation, as it simultaneously affects gas-liquid contact time and area. The inlet concentrations of both NO_2 and S(IV) substantially affect S(IV) oxidation, indicating a strong kinetically controlled oxidation reaction.

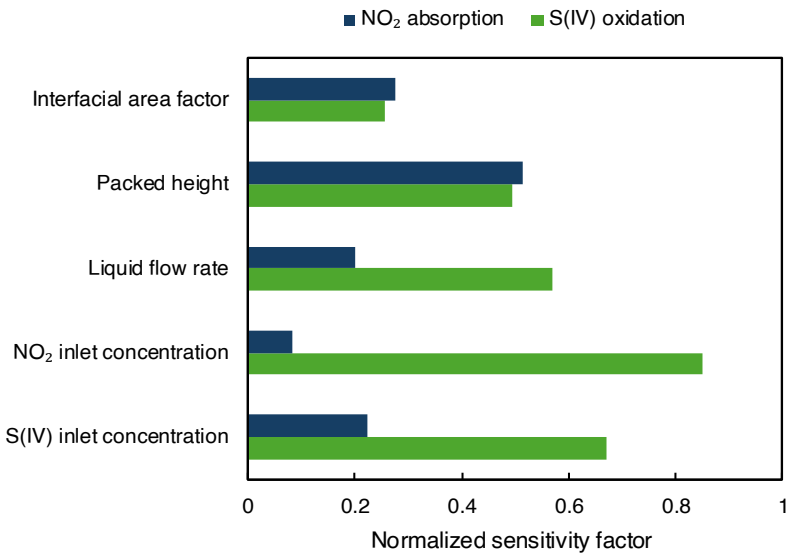

Figure 12 *Normalized sensitivity factors for NO_2 absorption and S(IV) oxidation for the various operating parameters.*

6 Conclusion

This thesis investigates the aqueous-phase chemistry governing the simultaneous absorption of NO_x and SO_x from flue gases, focusing on the oxidation of S(IV) in the presence of dissolved NO_2 and O_2 and the process of radical scavenging by thiosulfate. New reaction sets and their kinetic expressions are formulated by combining empirical data with kinetic modeling in **Paper I** and process modeling in **Paper II**. The proposed reactions are applied to evaluate process performance under various operating conditions. The main findings are summarized below.

- The rapid depletion of S(IV) observed during NO_2 absorption in a laboratory-scale setup is well described by both a radical-initiated reaction (SRR) and a global reaction (GRR). The rates of the radical chain reactions reveal that the chain propagation steps govern the consumption of S(IV), rather than the initiation by NO_2, which explains how a small amount of absorbed NO_2 can deplete a large amount of S(IV).

- Incorporating the global reaction into the process modeling software requires further adjustment of the rate expression, due to the substantial difference in concentration gradient between a laboratory-scale setup and an absorption column. Decoupling the S(IV) oxidation reaction and NO_2 absorption by assigning a high stoichiometric coefficient for SO_3^{2-} in the reaction $R_{N\text{-}S}$ gives a better representation of the rapid S(IV) consumption and its effect on NO_2 absorption in the column. In the closed-loop configuration, the models underestimate S(IV) consumption, which displays more-pronounced oxidation in the closed-loop setup.

- The thiosulfate scavenging mechanism reported in the literature (ThRX) can be reduced to a simplified set (ThRR). The negligible levels of regeneration of thiosulfate and polythionate formation confirm the suitability of the simplified reaction set. However, the model fails to predict the consumption of thiosulfate; a low level of consumption is observed in the experimental measurements.

- The sensitivity analysis results show that NO_2 absorption is governed by the amount of available S(IV), whereas S(IV) oxidation responds strongly to the inlet concentrations of both S(IV) and NO_2. This indicates that process performance is controlled primarily by the liquid-phase reactions that occur between the sulfur and nitrogen species. Furthermore, the influences of mass transfer parameters need to be considered when optimizing the process, as they exert a moderate effect on NO_2 absorption.

In summary, this work characterizes the mechanisms of NO_2-induced S(IV) oxidation and the process of radical scavenging by thiosulfate. The ability to reproduce measured liquid- and gas-phase concentrations confirms that the model captures the underlying chemistry in the system. The resulting prediction of S(IV) consumption allows the identification of key operating parameters, through which the high S(IV) demand can be managed. Evaluating the process across different setups creates the basis for more-reliable design and control as the process is scaled up. Together, these insights help to address the high chemical throughput that has so far constrained the absorption process.

7 Future work

The thesis proposed mechanisms that are evaluated against empirical measurements. However, given the broad operating conditions under which the process is applied, the following knowledge gaps are identified in relation to predicting and optimizing the combined removal of NO_x and SO_x:

- *Process behavior under various reactant concentrations.* Overestimation of the S(IV) oxidation at low inlet S(IV) concentrations indicates that the fitted rate constant of Reaction $R_{N\text{-}S}$ requires further examination across a broader range of inlet reactant concentrations. Thus, experiments that entail a broader set of S(IV) and NO_2 loadings would determine whether a single rate constant is adequate or whether a concentration-dependent description is required.

- *Refined radical scavenging mechanism model.* Here, thiosulfate consumption is not fully characterized, as its degradation over time is not captured in the present work. Furthermore, its scavenging performance is not in proportion to its concentration. This behavior is yet to be reflected in the proposed scavenging mechanism.

- *Process simulation involving a radical scavenger.* Thiosulfate plays a key role in sustaining the presence of S(IV), which allows for stable NO_2 absorption and significantly improved process viability. A global scavenging reaction needs to be developed that enables its integration into the process modeling software.

- *Inclusion of additional nitrogen oxide species.* The present mechanism assumes that NO_2 is the sole NO_x species entering the absorber. However, since different gas-phase oxidizing agents generate different distributions of NO_x species, extending the mechanism to include these species is essential.

Addressing these aspects would refine the application of the proposed mechanism as a predictive tool for process design and control, allowing further evaluations of the process feasibility and operating cost under realistic conditions. Beyond the absorption chemistry, an appropriate solution to liquid waste generation is necessary to achieve the intended environmental benefit of the technology. This challenge is beyond the scope of the present thesis and represents an important topic for future research.

References

(1) Manisalidis, I.; Stavropoulou, E.; Stavropoulos, A.; Bezirtzoglou, E., *Environmental and Health Impacts of Air Pollution: A Review.* Frontiers in Public Health, **2020**. 8.

(2) Javed, A.; Aamir, F.; Gohar, U.F.; Mukhtar, H.; Zia-UI-Haq, M.; Alotaibi, M.O.; Bin-Jumah, M.N.; Marc , R.A.; Pop, O.L., *The Potential Impact of Smog Spell on Humans' Health Amid COVID-19 Rages.* International Journal of Environmental Research and Public Health, **2021**. 18(21): p. 11408.

(3) Yang, L.E.; Hoffmann, P.; Scheffran, J., *Health impacts of smog pollution: the human dimensions of exposure.* The Lancet Planetary Health, **2017**. 1(4): p. e132-e133.

(4) Prakash, J.; Agrawal, S.B.; Agrawal, M., *Global Trends of Acidity in Rainfall and Its Impact on Plants and Soil.* Journal of Soil Science and Plant Nutrition, **2023**. 23(1): p. 398-419.

(5) McDuffie, E.E.; Smith, S.J.; O'Rourke, P.; Tibrewal, K.; Venkataraman, C.; Marais, E.A.; Zheng, B.; Crippa, M.; Brauer, M.; Martin, R.V., *A global anthropogenic emission inventory of atmospheric pollutants from sector- and fuel-specific sources (1970–2017): an application of the Community Emissions Data System (CEDS).* Earth System Science Data, **2020**. 12(4): p. 3413-3442.

(6) Kurokawa, J.; Ohara, T., *Long-term historical trends in air pollutant emissions in Asia: Regional Emission inventory in ASia (REAS) version 3.* Atmospheric Chemistry and Physics, **2020**. 20(21): p. 12761-12793.

(7) European Environment Agency, *Air pollution in Europe: 2023 reporting status under the National Emission reduction Commitments Directive.* 2023.

(8) U.S. Environmental Protection Agency. *Power Sector Evolution*. 2025 April 7, 2025]; Available from: https://www.epa.gov/power-sector/power-sector-evolution#powersectortrends.

(9) Ren, X.; Sun, R.; Meng, X.; Vorobiev, N.; Schiemann, M.; Levendis, Y.A., *Carbon, sulfur and nitrogen oxide emissions from combustion of pulverized raw and torrefied biomass.* Fuel, **2017**. 188: p. 310-323.

(10) Zel'dovich, Y.B., *Acta Physicochimica U.R.S.S.* **1946**. 11: p. 577-628.

(11) Wang, Z.; Yang, X., *NOx Formation Mechanism and Emission Prediction in Turbulent Combustion: A Review.* Applied Sciences, **2024**. 14(14): p. 6104.

(12) International Energy Agency, *Renewables 2024: Analysis and forecast to 2030*. 2024.

(13) International Energy Agency, *Global Hydrogen Review 2024*. 2024.

(14) Lecomte, T.; Ferreria de la Fuente, J.F.; Neuwahl, F.; Canova, M.; Pinasseau, A.; Jankov, I.; Brinkmann, T.; Roudier, S.; Delgado Sancho, L., *Best Available Techniques (BAT) Reference Document for Large Combustion Plants*, in *Industrial Emissions Directive 2010/75/EU (Integrated Pollution Prevention and Control)*. 2017, Joint Research Centre, European Commission.

(15) OECD, *Best Available Techniques (BAT) for Preventing and Controlling Industrial Pollution, Activity 6: Cross Country analysis of BAT and BAT-associated emission and environmental performance levels in the Thermal Power Plants, Cement and Textile industries*, in *OECD Series on Risk Management*. 2022, Environment Directorate, OECD: Paris.

(16) Damma, D.; Ettireddy, P.R.; Reddy, B.M.; Smirniotis, P.G. *A Review of Low Temperature NH3-SCR for Removal of NOx*. Catalysts, **2019**. 9, DOI: 10.3390/catal9040349.

(17) Staudt, J.E., *Minimizing the Impact of SCR Catalyst on Total Generating Cost Through Effective Catalyst Management*. 2004. p. 731-740.

(18) Takeuchi, H.; Takahashi, K.; Kizawa, N., *Absorption of Nitrogen Dioxide in Sodium Sulfite Solution from Air as a Diluent.* Industrial & Engineering Chemistry Process Design and Development, **1977**. 16(4): p. 486-490.

(19) Sun, Y.; Zwolińska, E.; Chmielewski, A.G., *Abatement technologies for high concentrations of NOx and SO2 removal from exhaust gases: A review.* Critical Reviews in Environmental Science and Technology, **2016**. 46(2): p. 119-142.

(20) Si, M.; Shen, B.; Adwek, G.; Xiong, L.; Liu, L.; Yuan, P.; Gao, H.; Liang, C.; Guo, Q., *Review on the NO removal from flue gas by oxidation methods.* Journal of Environmental Sciences, **2021**. 101: p. 49-71.
(21) Ytreberg, E.; Hassellöv, I.-M.; Nylund, A.T.; Hedblom, M.; Al-Handal, A.Y.; Wulff, A., *Effects of scrubber washwater discharge on microplankton in the Baltic Sea.* Marine Pollution Bulletin, **2019**. 145: p. 316-324.
(22) Teuchies, J.; Cox, T.J.S.; Van Itterbeeck, K.; Meysman, F.J.R.; Blust, R., *The impact of scrubber discharge on the water quality in estuaries and ports.* Environmental Sciences Europe, **2020**. 32(1): p. 103.
(23) Johansson, J.; Heijnesson Hultén, A.; Normann, F.; Andersson, K., *Simultaneous Removal of NOx and SOx from Flue Gases Using ClO2: Process Scaling and Modeling Simulations.* Industrial & Engineering Chemistry Research, **2021**. 60(4): p. 1774-1783.
(24) Sapkota, V.N.A.; Fine, N.A.; Rochelle, G.T., *NO2-Catalyzed Sulfite Oxidation.* Industrial & Engineering Chemistry Research, **2015**. 54(17): p. 4815-4822.
(25) Littlejohn, D.; Wang, Y.; Chang, S.G., *Oxidation of aqueous sulfite ion by nitrogen dioxide.* Environmental Science & Technology, **1993**. 27(10): p. 2162-2167.
(26) Shen, C.H.; Rochelle, G.T., *Nitrogen Dioxide Absorption and Sulfite Oxidation in Aqueous Sulfite.* Environmental Science & Technology, **1998**. 32(13): p. 1994-2003.
(27) Yagi, S.; Inoue, H., *The absorption of oxygen into sodium sulphite solution.* Chemical Engineering Science, **1962**. 17(6): p. 411-421.
(28) Beilke, S.; Lamb, D.; Müller, J., *On the uncatalyzed oxidation of atmospheric SO2 by oxygen in aqueous systems.* Atmospheric Environment (1967), **1975**. 9(12): p. 1083-1090.
(29) Clifton, C.L.; Altstein, N.; Huie, R.E., *Rate constant for the reaction of nitrogen dioxide with sulfur(IV) over the pH range 5.3-13.* Environmental Science & Technology, **1988**. 22(5): p. 586-589.
(30) Schmid, D.; Hupa, M.; Paavola, M.; Vuorinen, I.; Lehikoinen, A.; Karlström, O., *Role of Thiosulfate in NO2 Absorption in Aqueous Sulfite Solutions.* Industrial & Engineering Chemistry Research, **2023**. 62(1): p. 105-110.
(31) World Health Organization, *Sustainable Development Goal indicator 3.9.1: mortality attributed to air pollution*. 2024, World Health Organization: Geneva.
(32) Schraufnagel, D.E.; Balmes, J.R.; Cowl, C.T.; De Matteis, S.; Jung, S.H.; Mortimer, K.; Perez-Padilla, R.; Rice, M.B.; Riojas-Rodriguez, H.; Sood, A.; Thurston, G.D.; To, T.; Vanker, A.; Wuebbles, D.J., *Air Pollution and Noncommunicable Diseases: A Review by the Forum of International Respiratory Societies' Environmental Committee, Part 2: Air Pollution and Organ Systems.* Chest, **2019**. 155(2): p. 417-426.
(33) European Environment Agency, *Unequal exposure and unequal impacts: social vulnerability to air pollution, noise and extreme temperatures in Europe*. 2018, Publications Office of the European Union: Luxembourg.
(34) World Health Organization, *WHO global air quality guidelines: particulate matter (PM2.5 and PM10), ozone, nitrogen dioxide, sulfur dioxide and carbon monoxide*. 2021, World Health Organization: Geneva.
(35) Chameides, W.; Walker, J.C.G., *A photochemical theory of tropospheric ozone.* Journal of Geophysical Research (1896-1977), **1973**. 78(36): p. 8751-8760.
(36) Calvert, J.; Stockwell, W., *Mechanism and rates of the gas phase oxidations of sulfur dioxide and the nitrogen oxides in the atmosphere*, in *SO_2, NO and NO_2 oxidation mechanisms: atmospheric considerations*. 1983, Butterworth Publishers: Boston, MA.
(37) Basith, S.; Manavalan, B.; Shin, T.H.; Park, C.B.; Lee, W.S.; Kim, J.; Lee, G., *The Impact of Fine Particulate Matter 2.5 on the Cardiovascular System: A Review of the Invisible Killer.* Nanomaterials (Basel), **2022**. 12(15).
(38) Clark, C.M.; Bell, M.D.; Boyd, J.W.; Compton, J.E.; Davidson, E.A.; Davis, C.; Fenn, M.E.; Geiser, L.; Jones, L.; Blett, T.F., *Nitrogen-induced terrestrial eutrophication: cascading effects and impacts on ecosystem services.* Ecosphere, **2017**. 8(7): p. e01877.
(39) Driscoll, C.T.; Wang, Z., *Ecosystem Effects of Acidic Deposition*, in *Encyclopedia of Water*, P. Maurice, Editor. 2019, Wiley. p. 1-12.

(40) Hoesly, R.M.; Smith, S.; Prime, N.; Ahsan, H., *A global anthropogenic emissions inventory of reactive gases and aerosols (1750 - 2023): an update to the Community Emissions Data System (CEDS)*, in *AGU Fall Meeting Abstracts*. 2024: Washington, D.C. p. GC23F-0316.
(41) U.S. Environmental Protection Agency, *National Tier 1 CAPS Trends*. 2025, U.S. Environmental Protection Agency: Washington, DC.
(42) International Energy Agency, *Global EV Outlook 2025*. 2025, IEA: Paris.
(43) Directive 2009/30/EC, *Directive 2009/30/EC of the European Parliament and of the Council*. 2009: European Union. p. 88-113.
(44) U.S. Environmental Protection Agency, *Control of Emissions of Air Pollution from Nonroad Diesel Engines and Fuel; Final Rule.* **2004**. 69(124): p. 38958-39273.
(45) U.S. Environmental Protection Agency, *Control of Air Pollution from Motor Vehicles: Tier 3 Motor Vehicle Emission and Fuel Standards; Final Rule.* **2014**. 79(81): p. 23414-23886.
(46) International Maritime Organization. *Historic Background*. 2026-06-17; Available from: https://www.imo.org/en/ourwork/environment/pages/historic-background-.aspx.
(47) International Maritime Organization, *International Convention for the Prevention of Pollution from Ships (MARPOL)*. 1973, International Maritime Organization.
(48) Comer, B.; McCabe, S.; Carr, E.W.; Elling, M.; Sturrup, E.; Knudsen, B.; Beecken, J.; Winebrake, J.J., *Real-world NOx emissions from ships and implications for future regulations*. 2023, International Council on Clean Transportation (ICCT): Washington, DC.
(49) Miller, J.A.; Bowman, C.T., *Mechanism and modeling of nitrogen chemistry in combustion.* Progress in Energy and Combustion Science, **1989**. 15(4): p. 287-338.
(50) Remus, R.; Aguado-Monsonet, M.A.; Roudier, S.; Delgado Sancho, L., *Best Available Techniques (BAT) Reference Document for Iron and Steel Production*, in *JRC Reference Reports*. 2013, Publications Office of the European Union: Luxembourg.
(51) Schorcht, F.; Kourti, I.; Scalet, B.M.; Roudier, S.; Delgado Sancho, L., *Best Available Techniques (BAT) Reference Document for the Production of Cement, Lime and Magnesium Oxide*, in *JRC Reference Reports*. 2013, Publications Office of the European Union: Luxembourg.
(52) U.S. Environmental Protection Agency, *Standards of Performance for New Stationary Sources*, in *Code of Federal Regulations*. U.S. Government Publishing Office: Washington, DC.
(53) U.S. Environmental Protection Agency, *Sulfur Dioxide Allowance System*, in *Code of Federal Regulations*. U.S. Government Publishing Office: Washington, DC.
(54) Bo, X.; Jia, M.; Xue, X.; Tang, L.; Mi, Z.; Wang, S.; Cui, W.; Chang, X.; Ruan, J.; Dong, G.; Zhou, B.; Davis, S.J., *Effect of strengthened standards on Chinese ironmaking and steelmaking emissions.* Nature Sustainability, **2021**. 4(9): p. 811-820.
(55) Ministry of Ecology Environment of the People's Republic of China, *Opinions on Promoting the Implementation of Ultra-Low Emissions in the Iron and Steel Industry*. 2019, Ministry of Ecology and Environment of the People's Republic of China: Beijing, China.
(56) U.S. Environmental Protection Agency, *Natural Gas Combustion*. 1998, U.S. Environmental Protection Agency, Office of Air Quality Planning and Standards: Research Triangle Park, NC.
(57) Wright, M.L.; Lewis, A.C., *Emissions of NOx from blending of hydrogen and natural gas in space heating boilers.* Elementa: Science of the Anthropocene, **2022**. 10(1).
(58) Scalet, B.M.; Garcia Muñoz, M.; Sissa, A.Q.; Roudier, S.; Delgado Sancho, L., *Best Available Techniques (BAT) Reference Document for the Manufacture of Glass*, in *Industrial Emissions Directive 2010/75/EU (Integrated Pollution Prevention and Control)*. 2013, Publications Office of the European Union: Luxembourg.
(59) Koech, L.; Rutto, H.; Lerotholi, L.; Everson, R.C.; Neomagus, H.; Branken, D.; Moganelwa, A., *Spray drying absorption for desulphurization: a review of recent developments.* Clean Technologies and Environmental Policy, **2021**. 23(6): p. 1665-1686.
(60) Richter, E., *BF/UHDE/MITSUI-Active Coke Process for Simultaneous SO2- and NOx-Removal*, in *Sulphur Dioxide and Nitrogen Oxides in Industrial Waste Gases: Emission, Legislation and Abatement*, D. van Velzen, Editor. 1991, Springer Netherlands: Dordrecht. p. 157-166.

(61) U.S. Department of Energy, N.E.T.L., *SNOX™ Flue Gas Cleaning Demonstration Project: A DOE Assessment*. 2000, U.S. Department of Energy, National Energy Technology Laboratory: Morgantown, WV.
(62) Ohlms, N., *DESONOX process for flue gas cleaning.* Catalysis Today, **1993**. 16(2): p. 247-261.
(63) Kudlac, G.A.; Farthing, G.A.; Szymanski, T.; Corbett, R., *SNRB catalytic baghouse laboratory pilot testing.* Environmental Progress, **1992**. 11(1): p. 33-38.
(64) Gao, S.; Nakagawa, N.; Kato, K.; Inomata, M.; Tsuchiya, F., *Simultaneous SO2/NOx removal by a powder-particle fluidized bed.* Catalysis Today, **1996**. 29(1): p. 165-169.
(65) Pennline, H.W.; Hoffman, J.S., *Flue gas cleanup using the Moving-Bed Copper Oxide Process.* Fuel Processing Technology, **2013**. 114: p. 109-117.
(66) Bolli, R.E.; Woods, M.C.; Madden, D.R.; Corfman, D.W., *Noxso: A No-Waste Emission Control Technology*, in *Coal Science and Technology*, B.K. Parekh and J.G. Groppo, Editors. 1993, Elsevier. p. 437-449.
(67) Wilde, J.D.; Marin, G.B., *Investigation of simultaneous adsorption of SO2 and NOx on Na-γ-alumina with transient techniques.* Catalysis Today, **2000**. 62(4): p. 319-328.
(68) Park, J.-H.; Ahn, J.-W.; Kim, K.-H.; Son, Y.-S., *Historic and futuristic review of electron beam technology for the treatment of SO2 and NOx in flue gas.* Chemical Engineering Journal, **2019**. 355: p. 351-366.
(69) Basfar, A.A.; Fageeha, O.I.; Kunnummal, N.; Al-Ghamdi, S.; Chmielewski, A.G.; Licki, J.; Pawelec, A.; Tymiński, B.; Zimek, Z., *Electron beam flue gas treatment (EBFGT) technology for simultaneous removal of SO2 and NOx from combustion of liquid fuels.* Fuel, **2008**. 87(8): p. 1446-1452.
(70) Ighigeanu, D.; Martin, D.; Zissulescu, E.; Macarie, R.; Oproiu, C.; Cirstea, E.; Iovu, H.; Calinescu, I.; Iacob, N., *SO2 and NOx removal by electron beam and electrical discharge induced non-thermal plasmas.* Vacuum, **2005**. 77: p. 493-500.
(71) Chang, M.B.; Lee, H.M.; Wu, F.; Lai, C.R., *Simultaneous removal of nitrogen oxide/nitrogen dioxide/sulfur dioxide from gas streams by combined plasma scrubbing technology.* Journal of the Air & Waste Management Association, **2004**. 54(8): p. 941-9.
(72) Du, C.; Yi, H.; Tang, X.; Zhao, S.; Gao, F.; Yu, Q.; Yang, Z.; Yang, K.; Xie, X.; Ma, Y., *Desulfurization and denitrification experiments in SDA system: A new high-efficient semi-dry process by NaClO2.* Separation and Purification Technology, **2020**. 230: p. 115873.
(73) Cai, M.; Liu, X.; Zhu, T.; Zou, Y.; Tao, W.; Tian, M., *Simultaneous removal of SO2 and NO using a spray dryer absorption (SDA) method combined with O3 oxidation for sintering/pelleting flue gas.* Journal of Environmental Sciences, **2020**. 96: p. 64-71.
(74) Zhao, Y.; Han, Y.; Ma, T.; Guo, T., *Simultaneous Desulfurization and Denitrification from Flue Gas by Ferrate(VI).* Environmental Science & Technology, **2011**. 45(9): p. 4060-4065.
(75) Zhu, T.; Xu, W.; Zhao, R.; Ye, M., *Equipment and method for circulating fluidized bed semidry simultaneous desulfurization, denitration, demercuration, and removal of dioxins of sintering flue gas*. 2016, Institute of Process Engineering, Chinese Academy of Sciences; Beijing ZSTC Environmental Engineering Co., Ltd.: China.
(76) Ma, Q.; Wang, Z.; Lin, F.; Kuang, M.; Whiddon, R.; He, Y.; Liu, J., *Characteristics of O3 Oxidation for Simultaneous Desulfurization and Denitration with Limestone–Gypsum Wet Scrubbing: Application in a Carbon Black Drying Kiln Furnace.* Energy & Fuels, **2016**. 30(3): p. 2302-2308.
(77) BOC Process Gas Solutions, *Low Temperature Oxidation System Demonstration at RSR Quemetco, Inc., City of Industry, California: Final Report*. 2001, California Air Resources Board, Innovative Clean Air Technology Program: Sacramento, CA.
(78) Hutson, N.D.; Krzyzynska, R.; Srivastava, R.K., *Simultaneous Removal of SO2, NOx, and Hg from Coal Flue Gas Using a NaClO2-Enhanced Wet Scrubber.* Industrial & Engineering Chemistry Research, **2008**. 47: p. 5825-5831.
(79) Chin, T.; Tam, I.C.K.; Yin, C.-Y., *Comparison of various chemical compounds for the removal of SO2 and NOx with wet scrubbing for marine diesel engines.* Environmental Science and Pollution Research, **2022**. 29(6): p. 8873-8891.

(80) Johansson, J.; Heijnesson Hultén, A.; Normann, F.; Andersson, K., *Simultaneous Removal of NOx and SOx from Flue Gases Using ClO2: Process Scaling and Modeling Simulations.* Industrial & Engineering Chemistry Research, **2021**. 60: p. 1774-1783.
(81) Guo, S.; Lv, L.; Zhang, J.; Chen, X.; Tong, M.; Kang, W.; Zhou, Y.; Lu, J., *Simultaneous removal of SO2 and NOx with ammonia combined with gas-phase oxidation of NO using ozone.* Chemical Industry and Chemical Engineering Quarterly, **2015**. 21(2): p. 305-310.
(82) Murciano, L.T.; et al., *Study of individual reactions of the sour-compression process for the purification of oxyfuel-derived CO2.* International Journal of Greenhouse Gas Control, **2011**.
(83) White, V.; Wright, A.; Tappe, S.; Yan, J., *The Air Products / Vattenfall oxyfuel CO2 compression and purification pilot plant at Schwarze Pumpe.* Energy Procedia, **2013**. 37: p. 1490.
(84) Mochida, I.; Korai, Y.; Shirahama, M.; Kawano, S.; Hada, T.; Seo, Y.; Yoshikawa, M.; Yasutake, A., *Removal of SOx and NOx over activated carbon fibers.* Carbon, **2000**. 38: p. 227-239.
(85) Zhang, J.; Zhang, R.; Chen, X.; Tong, M.; Kang, W.; Guo, S.; Zhou, Y.; Lu, J., *Simultaneous removal of NO and SO2 from flue gas by ozone oxidation and NaOH absorption.* Industrial & Engineering Chemistry Research, **2014**. 53: p. 6450-6456.
(86) Johansson, J.; Heijnesson Hultén, A.; Ajdari, S.; Nilsson, P.; Samuelsson, M.; Normann, F.; Andersson, K., *Gas-Phase Chemistry of the NO–SO2–ClO2 System Applied to Flue Gas Cleaning.* Industrial & Engineering Chemistry Research, **2018**. 57(43): p. 14347-14354.
(87) Collins, M.M.; Cooper, C.D.; Dietz, J.D.; III, C.A.C.; Tazi, L.M., *Pilot-Scale Evaluation of H2O2 Injection to Control NOx Emissions.* Journal of Environmental Engineering, **2001**. 127(4): p. 329-336.
(88) Zhao, Y.; Hao, R.L., *Denitrification utilizing a vaporized enhanced-Fenton reagent: kinetics and feasibility.* RSC Advances, **2014**. 4: p. 46060-46067.
(89) Hao, R.L.; Zhao, Y., *Macrokinetics of NO oxidation by vaporized H2O2 in association with ultraviolet light.* Energy & Fuels, **2016**. 30: p. 2365-2372.
(90) Bai, M.; Zhang, Z.; Bai, M., *Simultaneous desulfurization and denitrification of flue gas by ·OH radicals produced from O2+ and water vapor in a duct.* Environmental Science & Technology, **2012**. 46(18): p. 10161-8.
(91) Wang, Z.; Lun, L.; Tan, Z.; Zhang, Y.; Li, Q., *Simultaneous wet desulfurization and denitration by an oxidant absorbent of NaClO2/CaO2.* Environmental Science and Pollution Research, **2019**. 26(28): p. 29032-29040.
(92) Hao, R.L.; Yang, S.; Yuan, B.; Zhao, Y., *Simultaneous desulfurization and denitrification through an integrative process utilizing NaClO2/Na2S2O8.* Fuel Processing Technology, **2017**. 159: p. 145.
(93) Jin, D.S.; Deshwal, B.R.; Park, Y.S.; Lee, H.K., *Simultaneous removal of SO2 and NO by wet scrubbing using aqueous chlorine dioxide solution.* Journal of Hazardous Materials, **2006**.
(94) Adewuyi, Y.G.; Sakyi, N.Y.; Arif Khan, M., *Simultaneous removal of NO and SO2 from flue gas by combined heat and Fe2+ activated aqueous persulfate solutions.* Chemosphere, **2018**. 193: p. 1216-1225.
(95) Liu, Y.; Wang, Y.; Xu, W.; Yang, W.; Pan, Z.; Wang, Q., *Simultaneous absorption–oxidation of nitric oxide and sulfur dioxide using ammonium persulfate synergistically activated by UV-light and heat.* Chemical Engineering Research and Design, **2018**. 130: p. 321-333.
(96) Chu, H.; Chien, T.W.; Li, S.Y., *Simultaneous absorption of SO2 and NO from flue gas with KMnO4/NaOH solutions.* Science of The Total Environment, **2001**. 275(1): p. 127-135.
(97) White, V.; Torrente-Murciano, L.; Sturgeon, D.; Chadwick, D., *Purification of oxyfuel-derived CO2.* International Journal of Greenhouse Gas Control, **2010**. 4(2): p. 137-142.
(98) Li, X.; Huang, Q.; Luo, C.; Zhang, Z.; Xu, Y.; Zhang, L.; Zheng, C., *Effects of acidic gases and operation parameters on denitrification in oxy-fuel CO2 compression process.* Fuel, **2018**. 234: p. 1285-1292.
(99) Cheng, Q.; Li, W.; Liu, D.; Chen, J.; Yang, H.; Jin, J., *Simultaneous Absorption of NOx and SO2 into Water and Acids under High Pressures.* Energy & Fuels, **2020**. 34(8): p. 9787-9795.

(100) Ajdari, S.; Normann, F.; Andersson, K.; Johnsson, F., *Reduced Mechanism for Nitrogen and Sulfur Chemistry in Pressurized Flue Gas Systems.* Industrial & Engineering Chemistry Research, **2016**. 55(19): p. 5514-5525.
(101) Harned, H.S.; Davis, R., Jr., *The Ionization Constant of Carbonic Acid in Water and the Solubility of Carbon Dioxide in Water and Aqueous Salt Solutions from 0 to 50°.* Journal of the American Chemical Society, **1943**. 65(10): p. 2030-2037.
(102) Mo, J.-s.; Wu, Z.-b.; Cheng, C.-j.; Guan, B.-h.; Zhao, W.-r., *Oxidation inhibition of sulfite in dual alkali flue gas desulfurization system.* Journal of Environmental Sciences, **2007**. 19(2): p. 226-231.
(103) Johansson, J.; Wagaarachchige, J.D.; Normann, F.; Idris, Z.; Haugen, E.R.; Halstensen, M.; Jinadasa, W.; Jens, K.J.; Andersson, K., *Influence of Nitrogen Dioxide Absorption on the Sulfite Oxidation Rate in the Presence of Oxygen: Online Raman Measurements.* Industrial & Engineering Chemistry Research, **2023**. 62(49): p. 21048-21056.
(104) Arriola, L.; Hyman, J.M., *Sensitivity Analysis for Uncertainty Quantification in Mathematical Models*, in *Mathematical and Statistical Estimation Approaches in Epidemiology*, G. Chowell, et al., Editors. 2009, Springer Netherlands: Dordrecht. p. 195-247.
(105) Fuller, E.C.; Crist, R.H., *The Rate of Oxidation of Sulfite Ions by Oxygen.* Journal of the American Chemical Society, **1941**. 63(6): p. 1644-1650.
(106) Schroeter, L.C., *Kinetics of Air Oxidation of Sulfurous Acid Salts.* Journal of Pharmaceutical Sciences, **1963**. 52(6): p. 559-563.
(107) Brimblecombe, P.; Spedding, D.J., *The catalytic oxidation of micromolar aqueous sulphur dioxide—I: Oxidation in dilute solutions containing iron (III).* Atmospheric Environment (1967), **1974**. 8(9): p. 937-945.
(108) Connick, R.E.; Zhang, Y.-X.; Lee, S.; Adamic, R.; Chieng, P., *Kinetics and Mechanism of the Oxidation of HSO3- by O2. 1. The Uncatalyzed Reaction.* Inorganic Chemistry, **1995**. 34(18): p. 4543-4553.